Treg-targeted IL-2/anti-IL-2 complex controls graft-versus-host disease and supports anti-tumor effect in allogeneic hematopoietic stem cell transplantation

Allan Thiolat, Caroline Pilon, Pamela Caudana, Audrey Moatti, Nhu Hanh To, Christine Sedlik, Mathieu Leclerc, Sébastien Maury, Eliane Piaggio, José L Cohen

Treg-targeted IL-2/anti-IL-2 complex controls graft-*versus*-host disease and supports anti-tumor effect in allogeneic hematopoietic stem cell transplantation

Allan Thiolat,[1*] Caroline Pilon,[1,2*] Pamela Caudana,[3,4] Audrey Moatti,[1] Nhu Hanh To,[1] Christine Sedlik,[3,4] Mathieu Leclerc,[1,5] Sébastien Maury,[1,2,5] Eliane Piaggio[3,4#] and José L Cohen,[1,2*#]

*AT and CP co- first authors

[#]EP and JLC co-last authors

1. Univ Paris Est Créteil, INSERM U955, IMRB, F-94010 Créteil, France

2. AP-HP, Groupe hospitalo-universitaire Chenevier Mondor, Centre d'Investigation Clinique Biothérapie, Fédération hospitalo-Universitaire TRUE, F-94010 Créteil, France

3. INSERM U932, PSL Research University, Institute Curie Research Center, Paris, France.

4. Department of Translational Research, PSL Research University, Institut Curie Research Center, Paris, France.

5. AP-HP, Groupe Hospitalo-Universitaire Chenevier Mondor, Service d'Hématologie Clinique, F-94010 Créteil, France

Running head: Treg-targeted IL-2/anti-IL-2 complex sustains GVHD prevention and GVL effect

Corresponding author: José L. Cohen : jose.cohen@inserm.fr

Author contributions: AT, CP, EP and JLC designed the study; AT, CP, PC, CS performed experiments; AT, CP, PC, AM, ML, SM EP and JLC analyzed the data, AT, CP, EP and JLC wrote the first draft of the manuscript and all authors contributed in the final version.

Author's disclosures: There are no competing interests to declare for all authors expect for E.P. who is co-founder and consultant for Egle-TX.

Data-sharing statement. Data and protocols are available on request to corresponding author.

Word count. Abstract: 229 words; main manuscript 5006 words

Acknowledgments: We are grateful to the IMRB for providing access to their animal facility team and the flow cytometry platform team for their help.

Funding: Audrey Moatti received a PhD grant from the Université Paris-Est-Créteil (UPEC). This work was fully supported and funded by a common grant from the French Ministry of Health and The French National Cancer Institute to JLC (PRTK-2015).

Abstract

Modulating an immune response in opposite directions represents the holy grail in allogeneic hematopoietic stem cell transplantation (allo-HSCT) to avoid insufficient reactivity of donor T cells and hematologic malignancy relapse while controlling the potential development of graft-versus-host disease (GVHD), in which donor T cells attack the recipient's tissues. IL-2/anti-IL-2 complexes (IL2-Cxs) represents a therapeutic option to selectively accentuate or dampen the immune response.

In dedicated experimental models of allo-HSCT, including also human cells injected in immunodeficient NSG mice, we evaluated side-by-side the therapeutic effect of two IL-2Cxs designed either to boost regulatory T cells (Tregs) or alternatively to activate effector T cells (Teffs), on GVHD occurrence and tumor relapse. We also evaluated the effect of the complexes on the phenotype and function of immune cells in vivo.

Unexpectedly, both pro-Treg and pro-Teff IL-2Cxs prevented GVHD development. They both induced Treg expansion and reduced $CD8^+$ T cells numbers, compared to untreated mice. However, only mice treated with the pro-Treg IL-2Cx, showed a dramatic reduction of exhausted $CD8^+$ T cells, consistent with a potent anti-tumor effect. When evaluated on human cells, pro-Treg IL-2Cx also preferentially induced Treg expansion in vitro and in vivo, while allowing the development of a potent anti-tumor effect in NSG mice.

Our results demonstrated the clinical relevance of using a pro-Treg, but not a pro-Teff IL2/anti-IL-2 complex to modulate alloreactivity after HSCT, while promoting a GVL effect.

Introduction

Initially identified for its capacity to stimulate T cells in vitro, interleukine-2 (IL-2) has been used in the clinic for boosting effector immune responses for the treatment of metastatic melanoma and renal carcinoma [1], or for inducing remission maintenance in patients with acute myeloid leukemia [2], although with limited (5-15% of responder patients) or non-significant benefit, respectively. Additionally, high-dose IL-2 administration is limited by its high associated toxicity.

Low efficacy of IL-2 in cancer can be explained by (i) an insufficient activation of $CD8^+$ T and NK cells, which respond to IL-2 through the intermediate affinity IL-2 receptor, composed of IL-2Rβ and IL-2Rγc [3], and/or (ii) by the undesired activation of regulatory T cells (Tregs). Once activated by IL-2, Tregs block the anti-tumor immune response [4]. Tregs constitutively express the high affinity IL-2 receptor composed by three subunits: IL-2-Rα, IL-2Rβ and IL-2Rγc [4], giving them an advantage over other T cells in the consumption of IL-2, especially in environments with poor IL-2 content. Thus, although IL-2 has a pleiotropic activity, its major role is to favor Treg survival and suppressive functions[5]. Consequently, low efficacy of IL-2 treatment in cancer is mainly due to low response of $CD8^+$ T and NK cells expressing the intermediate affinity IL-2 receptor, as well as the unwanted effect of IL-2 on Tregs due to their constitutive high affinity IL-2 receptor expression.

Understanding of the effect of IL-2 on Treg has led to the design of IL-2-based immunosuppressive strategies targeting Treg. Thus, contrary to what was initially proposed, IL-2 administered at low dose represents a novel immunosuppressive drug for the treatment of autoimmune and inflammatory diseases, acting by Treg activation. Allogeneic hematopoietic stem cell transplantation (allo-HSCT) is a particularly interesting situation to test the therapeutic efficacy of IL-2. Indeed, the risk associated with insufficient reactivity between donor and recipient is the hematologic malignancy

relapse for which allo-HSCT has been performed initially. In this case, high-dose IL-2 therapy could accentuate the graft-versus-leukemia/tumor (GVL/GVT) response through expansion and activation of donor effector T cells. On the other hand, the major complication of allo-HSCT is the development of life-threatening graft-versus-host disease (GVHD), in which donor T cells attack the recipient's tissues [6]. In this situation, low-dose IL-2 therapy could lead to Treg expansion, and thus to GVHD inhibition. Before the paradoxical effect of IL-2 on the immune response was understood, the group of David Sachs [7-9] initially observed that 3 days of low-dose IL-2 administration controlled experimental GVHD, while preserving the GVL/GVT effects. At odds, Shin et al. [10] reported a lack of therapeutic effect of low-dose IL-2 in experimental GVHD. We also studied different preventive or curative approaches based on low-dose IL-2 administration +/- rapamycin, but did not observe any effect on GVHD, including in a model of xenogeneic GVHD using human cells administered to immunodeficient mice [11]. In humans, low-dose IL-2 therapy has been administered to dampen inflammation in GVHD [12-14], but with either no, limited, or yet non-evidenced clinical recuperation. In our models, as well as in healthy volunteers or in allo-HSCT patients, low-dose IL-2 administration induced an approximately 1.5-2-fold expansion of Tregs without activating conventional T cells (Tconv). This increase in Treg numbers was far away from the desired 20-fold needed to reach a 1:1 Treg:Tconv ratio and consequently, a protective effect of Tregs in experimental GVHD, as we and other previously observed [15-19]. Thus, it is actually difficult to conclude on the potential of sole IL-2 administration to prevent GVHD or to induce GVL/GVT effect. Overall, improvements on IL-2-based therapy are needed to increase therapeutic efficacy in both situations.

IL-2/anti-IL-2 complexes represent an alternative to enhance IL-2 therapeutic usefulness. Depending on the IL-2 mAb used to generate the IL-2/anti-IL-2 complexes, they can direct IL-2 action to either effector T cells or to Tregs [20]. Consequently, some

complexes induce dramatic antitumor responses by vigorously activating effector immune cells [21]. Other complexes show a selective effect on Treg expansion, resulting in immune response attenuation and autoimmune control [22]. In allo-HSCT, the possibility of modulating donor T-cell alloreactivity in both directions depending on the used complexes remains unsolved [23-26]. Moreover, no study has systematically compared the effect of different complexes side-by-side. Here, we tested two IL-2/anti-IL-2 complexes. One is made with a pro-Treg mAb (i.e., preferentially activating Tregs bearing the IL-2R$\alpha\beta\gamma$, now referred to as Cx25 as CD25 is the IL-2Rα chain). The mAb used in Cx25 binds to the part of IL-2 that normally binds to the IL-2R$\beta\gamma$. As a result, IL-2 effect will be mainly mobilized for Tregs that constitutively express CD25. The second one is made with a pro-T effector mAb (i.e., preferentially activating effector IL-2R$\beta\gamma$- bearing cells, such as $CD4^+$ conventional T cell, $CD8^+$ T cells and NK cells, now referred to as Cx122 as CD122 is the IL-2Rβ chain). The mAb used in Cx122 binds to the part of IL-2 that normally binds to the high affinity IL-2Rα. As a consequence, IL-2 lose its preferential affinity for constitutively-expressing CD25 Tregs, leading to an improved availability of IL-2 for conventional T cells. We show that even if both complexes are effective in preventing GVHD, only the pro-Treg complex allows the emergence of the GVL/GVT effect.

Methods

Mice and GVHD models

Female C57BL/6J (B6, H-2^{b}), BALB/cJ (H-2^{d}), (B6xDBA2) F1 (B6D2F1, H-2^{bxd}), (B6xC3H) F1 (B6C3F1, H-2^{bxk}) from Charles River Laboratories (France) were used at 8 to 10 weeks of age. NSG (NOD.Cg-Prkdc^{scid}IL2rg^{tm1Wjl}/SzJ) mice were obtained from our own breeding and used at 10–12 weeks of age. All experiment protocols were approved by the local ethics committee (authorization number N°APAFIS#11511-2017092610086943) and in compliance with European Union Guidelines.

GVHD was induced in B6C3F1 female injection of CD3+ T cells from B6 mice as previously described and evaluated three times a week[27,28].

Treatment

Recombinant human IL-2 (rhIL-2, Proleukine, Novartis), anti– CTLA4 (clone 9H10; Bio X Cell), anti-human IL-2 (clone MAB602; Bio-Techne), and anti-human IL-2 (clone 5344.111; BD Biosciences) were purchased. IL-2 complexes (IL-2Cx) were prepared by mixing 15,000 UI of rhIL-2 with 4.5 µg of mAb (molar ratio 2:1) and incubated for 30 minutes at 37°C. IL-2Cx is called Cx122 when made using MAB602 clone; and Cx25 when made using 5344.111 clone. IL-2Cx were administered in five or ten intraperitoneal injections from d0-d4 and d7-d11 or only from d0 to d4 after BMT according to experiments. Anti-CTLA-4 was administered in three intraperitoneal mAb injections of 200 µg each on d0, d3, and d6 after BMT.

Phenotypic analysis of immune cell populations

Spleens were harvested on day 12 and splenocytes stained with the antibodies listed in Supplemental Table 1. Non-specific binding was blocked using anti-CD16/CD32 (Miltenyi Biotec). For intracellular cytokine staining, cells were stimulated for 5h with phorbol 12-myristate 13-acetate (PMA) 50ng/ml and ionomycin 1µg/ml (Sigma–Aldrich, Saint Louis, CA, USA,). Brefeldin A (BD Pharmingen, San Diego, CA, USA)

was added for the last 4 h. Then, cells were fixed and permeabilized with fixation/permeabilization solution (ThermoFischer), following the manufacturer's instructions. Data acquired with a Canto 2 flow cytometer were compensated and exported into FlowJo (version 10.0.8, TreeStar Inc).

Tumor relapse models

Irradiated recipient B6D2F1 female mice received retro-orbital infusion of P815-GFP mastocytoma cells (2 x 10^4 per mouse) +/- BM and T cells. GVHD symptoms were evaluated three times per week. Blood samples were systematically collected at day 14 to identify the presence of tumor cells before tumor apparition at the eye, the site of injection. GFP^+ cells were detected by flow cytometry analysis. In addition to blood sampling, presence of an eye tumor was assessed daily. Mice found to have tumors were sacrificed as previously described [27-29].

RS4;11-GFP+ acute lymphoblastic cells were used to test the possibility for human cells to support a GVL effect in NSG mice. For this, 3 x 10^6 $CD3^+$ cells contained in PBMC from two healthy donor blood samples (Etablissement Francais du Sang, Créteil, France) and 0.5 x 10^6 RS4;11-GFP^+ were intravenously injected at day 0. Mice were treated with Cx25 for 5 days from d2 to d6. At d20 and d30, mice were randomly sacrificed, and bone marrow, spleen, blood and liver were harvested for the exploration of the presence of tumor cells by GFP detection by flow cytometry.

Short-term in vivo xenogeneic human lymphocyte activation.

NSG mice were used to compare the effect of IL-2 and Cx25 on human healthy donor immune cells in vivo. 12 x 10^6 $CD3^+$ cells among PBMC from two healthy donor blood samples were injected at day 0 in NSG mice. IL-2 and Cx25 were injected at d0, d1 and d2. After 5 days, their spleens were collected, and analyzed by flow cytometry.

Results

In allo-HSCT, clinical effects are determined by the timing and duration of Cx25 and Cx122 administration, rather than by the mAb used to generate the complexes.

We performed a series of experiments to evaluate the effects of Cx25 and Cx122 on GVHD development. When administered at the time of BMT, both IL-2Cxs reduced clinical manifestations of GVHD, and prolonged survival of grafted mice, compared to untreated mice or mice receiving low doses of IL-2 (Figure 1A). Thus, unexpectedly, Cx25 and Cx122 induced a similar preventive effect on GVHD development when administered at the time of BMT and for a short period. Using the same anti-IL-2 mAbs than in our study to generate IL-2Cxs, the distinct effector T cell activation of the Cx122 complex [30] or, the pro-Treg effect of Cx25 [31] were previously documented in other clinical settings. We thus questioned whether the indissociable effects observed in our hands with the two IL-2Cxs were due to the particular setting of allo-HSCT. We grafted B6D2F1 skins onto B6 recipient mice and treated them for 4 days, initiating the treatments at time of skin grafting. In untreated mice, skin grafts were rapidly rejected at day 10 as well as in IL-2 or in Cx122 treated mice. As expected, skin rejection was delayed only in mice treated with Cx25 (Supplemental figure 1). These results are in accordance with the dissociated clinical effects previously described with Cx25 or Cx122 and suggest that the similar protective effects observed in our experiments (Figure 1A) are exclusively due to the particular setting of allo-HSCT.

We then reproduced experiments of BMT but extending the duration of IL-2Cx administration from d0 to d11. It led not only to a loss of their protective effect observed with a short time treatment, but even to an accentuation of GVHD, and accelerated death (Figure 1B). Prolonged low-dose IL-2 administration did not induce any significant effect on GVHD control. Thus, during allo-HSCT, the timing and/or the

duration of IL-2Cx administration seem more important in determining the clinical effect than the different nature of the complexes. These results indicate that short-time administration of IL-2Cxs at the time of BMT is more effective than low-dose IL-2 and similarly alleviates GVHD independently of the mAb used to generate the complexes. Cx25 and CX122 are supposed to act on different target cells. However, these two complexes induced comparable effects on GVHD when administered preventively. A possibility to assess whether or not their respective effects depend on Treg is to eliminate them in vivo at the same time as the complexes are administered. For this, we took advantage of our recently published data [29] showing that the in vivo administration of an anti-CTLA4 mAb at time of BMT efficiently eliminated Tregs. We therefore tested the effect of the IL-2Cxs when Tregs are eliminated by an anti-CTLA4 treatment. In this experiment, both IL2-Cxs still fully prevented GVHD, whereas anti-CTLA4 worsened it. Interestingly, the protective effect of both IL-2Cxs was reduced when anti-CTLA4 was co-administered, suggesting at least a partial link between IL-2Cx effects on Treg and GVHD attenuation (Supplemental figure 2).

In allo-HSCT, both Cx25 and Cx122 treatments increase the proportion of Tregs

Next, we evaluated the biological effects of both IL-2Cxs on immune reconstitution. First, we assessed IL-2Cx effects on immune cell engraftment at d12 (Figure 2A), as by this time 4 out 21 (19%) mice had died in the untreated control group, 2 out 16 (12.5%) in the IL2-treated group, 3 out 16 (18%) in the Cx122 group, and none in the Cx25 group. By the time the mice were sacrificed, weight curves and clinical scores already differed according to treatment (Figure 2B). Thus, d12 appears to be a tipping point for GVHD. The frequencies of Tregs and Teffs of recipient mouse origin were only residual, with only few $CD4^+Foxp3^+$, $CD4^+Foxp3^-$ and $CD8^+Foxp3^-$ cells expressing the $H\text{-}2K^k$ recipient-type molecules at their surface being detected in untreated mice (Figure 2C). Administration of Cx122, and to a lesser extent of Cx25,

increased the percentage of recipient $CD4^+$ T cells ($Foxp3^+$ or $Foxp3^-$) which, however, remained in very small proportions in the spleen of treated mice. Thus, both complexes induced a slight decrease in the engraftment as evidenced by the persistence of a larger, although minor, proportion of cells of recipient's origin. Given this observation, we considered that cells collected at d12 were mainly of donor origin (between 95 and 100%) and consequently attested for the biologic and clinical effects observed with both IL-2Cxs.

Whereas the absolute numbers of total spleen cells or of T cells were not modified in Cx25 treated mice or slightly decreased for CD8 T cells in Cx122 treated mice compared to untreated mice, we observed that the clinical immunosuppressive effects of both IL-2Cxs were compatible with the important decrease in CD8+ T cells percentage in Cx25 and Cx122 treated animals, compared to untreated mice; as well as with the increase of the proportion of CD4+Foxp3+ Tregs (Figure 3A and B). Comparable observations were made in the liver of grafted animals, a target organ of GVHD (Supplemental figure 3).

It has been previously observed that a small immunosuppressive $CD8^+Foxp3^+$ T cell population can emerge early during GVHD both in experimental models [32,33] and in humans [32,34]. Here, we observed that the frequency of spleen $CD8^+Foxp3^+$ T cells increased under IL-2Cx administration. Finally, we observed that the IL-2Cxs induced a dramatic reduction of the CD8/Treg ratios both in spleen and liver of grafted animals, likely underlying GVHD attenuation (Figure 3B and Supplemental figure 3B).

Then, we analyzed the expression of CTLA-4, CD25 and TNFR2 markers of Treg function and fitness (Supplemental figure 4) among the remaining $CD4^+$ $FOXP3^+$ Tregs. Although similar percentages of Tregs expressing CTLA-4 were observed, the mean fluorescence intensity (MFI) of CTLA-4 expression was statistically significantly increased after treatment with both IL-2Cxs. For CD25, only mice receiving Cx122

showed statistically significantly increased percentages of $CD25^+$ Tregs, with no major changes in its MFI values. Thus, the remaining Tregs in IL-2Cx-treated mice displayed a more activated phenotype, compatible with the observed reduced GVHD. However, this observation must be counterbalanced with the observed decrease in the percentage of Treg expressing TNFR2 in mice treated with the Cx25 (Supplemental figure 4).

The combined use of CD44 and CD62L membrane markers allows distinguishing naïve ($CD44^-CD62L^+$), memory effector ($CD44^+CD62L^-$) and central memory ($CD44^+CD62L^+$) T cells [35,36] (Supplemental figure 5A). Compared to untreated mice, Cx25 and Cx122 treatments dramatically increased the proportion of $CD4^+$ $Foxp3^-$ naïve T cells, whereas $CD4^+$ effector memory T cells were decreased. The proportion of $CD8^+$ effector memory T cells also decreased with Cx122, but not Cx25 administration. No major modification was observed in the central memory T cell compartment (Figure 4A). In the liver of grafted animals, $CD8^+$ effector memory T cells decreased and $CD8^+$ central memory T cells increased under Cx122 treatment (Supplemental Figure 6A).

Additionally, we evaluated the effects of complexes on the expression levels of the anergy/exhaustion T-cell markers PD-1, T-bet and Eomes (Supplemental figure 5B and C)[37,38]. Both IL-2Cxs induced a decrease in the percentage of splenic $CD4^+Foxp3^-$ and $CD8^+Foxp3^-$ PD-1-expressing conventional T cells and of liver $CD8^+Foxp3^-$ PD-1-expressing conventional T cells, suggesting a global attenuation of T cell activation, compared to untreated animals (Figure 4B and supplemental figure 6B). Among the 80% of $CD8^+Foxp3^-$ T cells that expressed PD-1, more than 70% co-expressed Eomes but not T-bet in untreated mice, attesting a very high fraction of potentially exhausted $CD8^+$ T cells. Interestingly, this fraction of cells dramatically dropped in mice treated with Cx25 (Figure 4C). The percentage of cells with the $Eomes^+T\text{-}bet^-$ phenotype

represented 20% of the $CD4^+PD\text{-}1^+$ cells and Cx122 treatment negatively impacted this cell population (Figure 4C). Thus, the effect of the complexes seems associated with a reduction in the percentage of activated effector T cells and a more marked and statistically significant decrease in the fraction of $CD8^+$ T cells with an exhausted phenotype when administering Cx25. Similar observations were made in the liver of grafted animals (Supplemental figure 5C).

IFNγ, TNFα and IL17 are considered as essential players during the cytokine storm associated with GVHD (Supplemental figure 7)[6]. We did not observe any major effects of both IL-2Cx treatments on cytokine production by effector T cells, except for IFNγ production by $CD8^+$ cells, with a statistically significant decrease only when Cx122 was used. The production of the three tested cytokines by Tregs statistically significantly decreased in Cx25 and Cx122 treated animals, compared to control group (Figure 5). Thus, as soon as d12, the inflammatory status of Tregs was dramatically modified when complexes were administered in grafted mice.

Cx25 but not Cx122 prevents GVHD while inducing a GVL/GVT effect

After observing that both complexes inhibit GVHD through different mechanisms of action, we evaluated their ability to induce a GVL effect. We used our recently published model in which BM cells ($5x10^6$ per mouse) are engrafted together with a defined number of tumor cells ($2x10^4$ P815-GFP cells per mouse) and T cells ($1x10^6$ $CD3^+$ T cell per mouse) into recipient mice, allowing tumor development without inducing GVHD. In this model, P815 tumors develop in 100% of mice, inexorably leading to 100% of tumor-related mortality by day 22, without the development of measurable clinical signs of GVHD (Figure 6A and B). We did not observe any differences in survival, tumor incidence or GVHD clinical grade in mice treated with Cx122, when compared to untreated mice. In marked contrast, Cx25 administration

led to the protection of half of the grafted mice from leukemia-induced death. No tumor cells were detected before day 20 and, over the duration of the experiment (d60), P815-GFP cells were detected only in 55% of the Cx25-treated mice. Interestingly, the anti-tumor effect in Cx25-treated mice was not associated to increased GVHD clinical score (Figure 6B). Thus, only Cx25, but not Cx122, induces a protective GVL effect in mice without inducing GVHD.

We recently showed in this same experimental model that anti-CTLA4, but not anti-PD-1 administration, induces a strong GVL effect, but is associated to lethal GVHD, rendering this therapeutic approach not compatible with a clinical use [29]. Thus, given that both IL-2Cx efficiently reduce GVHD, we hypothesized that their combination with anti-CTLA4 would represent an ideal situation associating the IL-2Cx GVHD-protective effect with the potent anti-tumor effect of anti-CTLA4 mAb. Combination of anti-CTLA4 with Cx122, did not improve mice survival, tumor incidence or GVHD clinical signs, compared to either IL-2Cx alone. However, the GVL/GVT effect as well as the improved survival obtained with Cx25 were lost when combined with anti-CTLA4 despite an increased alloreactivity, as attested by the statistically significant augmentation of the clinical grade compared to Cx25 alone (Figure 6B). This suggested that the GVL/GVT effect observed with Cx25 was not due to the sole alloreactivity, but rather to a yet non identified mechanism that could partially depend on CTLA4.

Preclinical considerations before Cx25 therapeutic utilization

Given that Cx25 was the sole IL-2Cx enabling GVHD control concomitant with GVL triggering, we assessed its effects on human immune cells in vitro and in a newly designed humanized mice model of leukemia. Of note, and for translational rational, this Cx25 is made of human IL-2 and anti-human IL-2 mAb. First, we co-cultured in

vitro $CD2^+$-sorted human cells containing T and NK cells with allogeneic APCs and evaluated the effects of IL-2 and Cx25 on cell proliferation (Supplemental figure 8). Addition of IL-2 induced a significant proliferation of $CD8^+$ and NK cells, but not of Tregs. At odds, Cx25 selectively increased the percentage of Tregs.

Next, we evaluated the effect of Cx25 on the initial steps of human T cell activation in vivo, five days after the adoptive transfer of human PBMCs containing 12 x 10^6 T cells into immunodeficient NSG mice (Figure 7A). At this time point, IL-2 or Cx25 administration did not modify the percentage of human colonizing immune cells (evaluated as percentage of human $CD45^+$ cells), in accordance with the similar levels of Ki67+ proliferating $CD4^+$ and $CD8^+$ T cells (Figure 7B). Of note, the percentage of Tregs strongly increased in mice treated with Cx25 compared to untreated or IL-2-treated mice. These results suggest that the protective effect of Cx25 evidenced by a preferential expansion of Treg is triggered very early after the adoptive transfer of human cells.

Even if the xeno-GVHD model, due to the high xeno-reactivity and the paucity of human cytokines and immune cell growth factors, only partially reflects the physiopathology of human GVHD, it is the only model allowing the in vivo evaluation of therapeutic molecules on human cells before clinical evaluation. This model is based on the administration in immunodeficient NSG mice of a number of human tumor cells mimicking a leukemia relapse and a suboptimal number of human T cells not allowing the development of an anti-leukemic effect. To evaluate the GVL effect of the Cx25, we infused NSG mice with the 0.5 x 10^6 RS4-GFP lymphoblast T cells, together with human PBMCs containing 3 x 10^6 T cells, and treated the mice with PBS or Cx25 for 5 consecutive days, starting on day 2 after cells injection (Figure 7C). When untreated mice were screened between d20 and d30 (a time line compatible with a leukemia development), RS4-GFP cells were detected in 6 out 8 untreated mice. In marked

contrast, no GFP-cells were detected in Cx25-treated mice, attesting of a potent GVL effect.

DISCUSSION

In this work, we comparatively analyzed the effects of IL-2Cxs made of two different anti-IL-2 mAbs with IL-2, with the aim to modulate the alloreactivity after allo-HSCT. Unexpectedly, both complexes, when administered early and for a short period, attenuated GVHD, resulting in prolonged mice survival in the absence of clinical signs of GVHD (Figure 1A). At odds with our data, the group of Bruce Blazar observed an acceleration of acute GVHD in Cx25-treated mice, and even an inhibition of the protective effect of transferred therapeutic Tregs [24]. These discordant results could be explained by the nature of the complexes (murine in their article, human in our work), but more probably by the level of histo-incompatibility between donor and recipient mice (fully allogeneic in Blazar et al, semi-allogeneic in our work). To confirm this hypothesis, we evaluated the effect of preventive treatment of Cx25 and Cx122 in a second B6 in BALB/c fully allogeneic model. No protective effect was observed (Supplemental figure 9A). Along these lines, they did observe the efficacy of the Cx25 complex, when used in the B6 into B10.BR chronic GVHD model.

In our model, administration of IL-2Cxs over a prolonged period of time, not only leads to a loss of their protective effects, but even accentuates GVHD development (Figure 1B). Because GVHD is a highly inflammatory pathology, it is likely that both complexes indiscriminately, activate Teffs more than Tregs when administered for a prolonged period, thus reflecting their loss of specificity of action. Indeed, we observed a strong increase in CD25 expression on a very high proportion of conventional T cells at d4 after transplantation, compared to those of donor T cells before their injection (Supplemental figure 9B). In accordance, IL-2Cx treatments initiated at day 5, when an elevated ratio of conventional T cells already strongly express CD25, has no protective effect on the occurrence of GVHD (Figure 9C). We therefore focused the

rest of this study on short treatments in order to understand the mechanisms of action of the two IL-2Cxs in HSCT and their potential clinical relevance.

The protective properties of both complexes were mainly associated with comparable biological effects on donor T cells (Figure 2B), inducing an efficient control of GVHD as the result of IL-2Cx effect at early time of BMT. In order to evaluate early events that complexes could have on Treg, we performed KI67 staining of donor T cells collected in grafted mice at day 4. First, we did not observe major difference on KI67 staining on Tregs depending on whether IL-2Cxs were administered or not. This suggested that at d4, treatments did not significantly influence the percentage of cycling Tregs. However, whereas each mouse was grafted with 2 x 10^5 Tregs at d0, the number of Treg collected at d4 in IL-2Cx-treated mice tended to increase compared to untreated mice. As the Treg viability were comparable (not shown), this suggested that IL-2Cxs likely induced Treg proliferation (Supplemental figure 9D).

It should be noted that $CD8^+Foxp3^+$ T cells appear during GVHD development, and increase in mice treated with both IL-2Cxs (Figure 3B), suggesting that $CD8^+$ Tregs arise with increased alloreactivity, as we and others have recently demonstrated [29,34,39]. Furthermore, $CD8^+$ Tregs represent an attractive therapeutic target since their frequencies are increased when GVHD is controlled. Along these lines, administration of a murine pro-Treg complex in combination with rapamycin was reported to expand $CD8^+Foxp3^+$ Treg cells with protective properties against GVHD [33]. Additionally, the controlled alloreactivity achieved by both IL-2Cxs could be attributed to a decrease of $CD4^+$ EM T cell frequencies, an increase of naive T cells, and a global decrease of T cell activation attested by reduced PD-1 expression by $CD4^+$ and $CD8^+$ T cells activation. Concerning Treg functions, both IL-2Cxs led to higher CTLA4 expression levels, without increasing the already high percentage of CTLA4-expressing Tregs (Supplemental Figure 2). In mice developing GVHD, Tregs atypically produced TNF-

α, IFN-γ and IL-17. Along these lines, it has been described that during autoimmune diseases Tregs can convert to pathological, dysregulated Tregs with reduced or no immunosuppressive properties [40,41]. Our results prone for IL-2Cxs likely halting this process of Treg dysregulation, thus ensuring the maintenance of their suppressive capacity (Figure 5).

IL-2Cxs also induced distinct effects on donor T cells. The statistically significant increase in the percentage of $CD25^+$ Tregs was only observed with the Cx122. Alternatively, the statistically significant decrease in TNFR2 expression was only observed with the Cx25 (supplemental figure 4). We have recently described that TNFR2 is essential for the suppressive functions of Tregs during allo-HSCT [27]. Thus, all these observations taken together, it could be concluded that GVHD is more efficiently controlled by Cx25, compared to Cx122. In Cx25-treated mice at d12, Tregs seem less mobilized to exert their suppressive effect which is reflected by their less activated/suppressive phenotype. This is consistent with discrete but noticeable differences observed between the two complexes, with the better probability of survival and the weaker clinical score (Figure 1A) obtained with Cx25 when compared to untreated mice ($p<0.001$), compared to those obtained with Cx122 ($p<0.005$). We also studied the $CD8^+PD\text{-}1^+EOMES^+T\text{-}bet^-$ T cell compartment that identifies an exhausted population of T cells. In GVHD-experiencing mice, it represents nearly 80% of $CD8^+$ T cells. Although Cx122 administration tended to reduce this cell population, only Cx25 induced a statistically significant decrease in the proportion of exhausted $CD8^+$ T cells. This observation may have important implications regarding the ability of donor cells to mediate a GVL/GVT effect. Indeed, when tumor cells were injected with T cells at the time of BMT, a GVT effect was only observed in mice that were concomitantly protected from GVHD by Cx25 administration. Importantly, this GVT effect was not associated with an increased clinical score of GVHD, suggesting that it could develop

partly independently of an increased alloreactivity. At odds, tumor cells were consistently detected in all untreated or Cx122 treated mice.

Overall, our study is the first, to our knowledge, to assess side by side the therapeutic effects of IL-2Cx on the occurrence of acute GVHD and the compatibility of such treatment with the development of a GVL/GVT effect. We demonstrate that only Cx25 effectively prevents GVHD while ensuring a GVL/GVT effect through a CTLA4-dependent mechanism. Indeed, co-administration of Cx25 and anti-CTLA4 was incompatible with the maintenance of a GVT effect, despite increased in alloreactivity. Our results are in accordance with the recent description of a method using an orthogonal IL-2/IL-2Rβ system targeting Tregs that allows to prevent GVHD while maintaining a GVL effect [42].

In this work, we made the choice to use human-compatible complexes in order to generate information that could be directly transferred to humans. We first demonstrated that these complexes can be evaluated in murine experimental GVHD. More importantly, this allowed us to directly test the Cx25 candidate complex on human cells, in vitro and in vivo. As observed in the whole murine mice model, Cx25 induced human Treg expansion in vitro at d2 and in vivo at d5 in NSG immunodeficient mice grafted with human PBMCs. In the same xeno-GVHD model, the co-injection of RS4 cells induced leukemia in 6 out of 8 mice between days 20 and 30, while no leukemic cells were detected when mice were treated with Cx25.

Taken together, our results demonstrate the clinical relevance of using complexes to modulate alloreactivity after HSCT. Due to its protective effects against GVHD and its capacity in inducing the GVL effect, our data sustains the use of Cx25 in a first clinical trial in patient with high-risk to develop GVHD. A secondary objective in these patients would be to assess the rate of leukemic relapse. It would be also interesting in this context to compare the effect of such complex with the direct in vivo injection of an

anti-IL-2 mAb, especially since two anti-IL-2 pro-Treg human mAbs have been described [43,44]. In this context, IL-2 Cxs have been described to be directly formed in vivo, and the efficacy of administration of a murine anti-IL-2 mAb in the prevention of GVHD has recently been demonstrated [25].

References

1. Rosenberg SA. Raising the bar: the curative potential of human cancer immunotherapy. *Sci Transl Med.* 2012;4(127):127ps128.
2. Buyse M, Squifflet P, Lange BJ, et al. Individual patient data meta-analysis of randomized trials evaluating IL-2 monotherapy as remission maintenance therapy in acute myeloid leukemia. *Blood.* 2011;117(26):7007-7013.
3. Malek TR. The biology of interleukin-2. *Annu Rev Immunol.* 2008;26:453-479.
4. Sakaguchi S, Sakaguchi N, Shimizu J, et al. Immunologic tolerance maintained by CD25+ CD4+ regulatory T cells: their common role in controlling autoimmunity, tumor immunity, and transplantation tolerance. *Immunol Rev.* 2001;182:18-32.
5. Papiernik M, de Moraes ML, Pontoux C, Vasseur F, Pénit C. Regulatory CD4 T cells: expression of IL-2R alpha chain, resistance to clonal deletion and IL-2 dependency. *Int Immunol.* 1998;10(4):371-378.
6. Ferrara JL, Levine JE, Reddy P, Holler E. Graft-versus-host disease. *Lancet.* 2009;373(9674):1550-1561.
7. Sykes M, Abraham VS, Harty MW, Pearson DA. IL-2 reduces graft-versus-host disease and preserves a graft-versus-leukemia effect by selectively inhibiting CD4+ T cell activity. *J Immunol.* 1993;150(1):197-205.
8. Sykes M, Romick ML, Sachs DH. Interleukin 2 prevents graft-versus-host disease while preserving the graft-versus-leukemia effect of allogeneic T cells. *Proc Natl Acad Sci U S A.* 1990;87(15):5633-5637.
9. Sykes M, Romick ML, Hoyles KA, Sachs DH. In vivo administration of interleukin 2 plus T cell-depleted syngeneic marrow prevents graft-versus-host disease mortality and permits alloengraftment. *J Exp Med.* 1990;171(3):645-658.
10. Shin HJ, Baker J, Leveson-Gower DB, Smith AT, Sega EI, Negrin RS. Rapamycin and IL-2 reduce lethal acute graft-versus-host disease associated with increased expansion of donor type CD4+CD25+Foxp3+ regulatory T cells. *Blood.* 2011;118(8):2342-2350.
11. Pérol L, Martin GH, Maury S, Cohen JL, Piaggio E. Potential limitations of IL-2 administration for the treatment of experimental acute graft-versus-host disease. *Immunol Lett.* 2014;162(2 Pt B):173-184.
12. Koreth J, Matsuoka K, Kim HT, et al. Interleukin-2 and regulatory T cells in graft-versus-host disease. *N Engl J Med.* 2011;365(22):2055-2066.
13. Kennedy-Nasser AA, Ku S, Castillo-Caro P, et al. Ultra low-dose IL-2 for GVHD prophylaxis after allogeneic hematopoietic stem cell transplantation mediates expansion of regulatory T cells without diminishing antiviral and antileukemic activity. *Clin Cancer Res.* 2014;20(8):2215-2225.
14. Ito S, Bollard CM, Carlsten M, et al. Ultra-low dose interleukin-2 promotes immune-modulating function of regulatory T cells and natural killer cells in healthy volunteers. *Mol Ther.* 2014;22(7):1388-1395.
15. Cohen JL, Trenado A, Vasey D, Klatzmann D, Salomon BL. CD4(+)CD25(+) immunoregulatory T Cells: new therapeutics for graft-versus-host disease. *J Exp Med.* 2002;196(3):401-406.

16. Trenado A, Charlotte F, Fisson S, et al. Recipient-type specific CD4+CD25+ regulatory T cells favor immune reconstitution and control graft-versus-host disease while maintaining graft-versus-leukemia. *J Clin Invest.* 2003;112(11):1688-1696.

17. Trenado A, Sudres M, Tang Q, et al. Ex vivo-expanded CD4+CD25+ immunoregulatory T cells prevent graft-versus-host-disease by inhibiting activation/differentiation of pathogenic T cells. *J Immunol.* 2006;176(2):1266-1273.

18. Kellner JN, Delemarre EM, Yvon E, et al. Third party, umbilical cord blood derived regulatory T-cells for prevention of graft versus host disease in allogeneic hematopoietic stem cell transplantation: feasibility, safety and immune reconstitution. *Oncotarget.* 2018;9(86):35611-35622.

19. Brunstein CG, Miller JS, Cao Q, et al. Infusion of ex vivo expanded T regulatory cells in adults transplanted with umbilical cord blood: safety profile and detection kinetics. *Blood.* 2011;117(3):1061-1070.

20. Boyman O, Kovar M, Rubinstein MP, Surh CD, Sprent J. Selective stimulation of T cell subsets with antibody-cytokine immune complexes. *Science.* 2006;311(5769):1924-1927.

21. Létourneau S, van Leeuwen EM, Krieg C, et al. IL-2/anti-IL-2 antibody complexes show strong biological activity by avoiding interaction with IL-2 receptor alpha subunit CD25. *Proc Natl Acad Sci U S A.* 2010;107(5):2171-2176.

22. Webster KE, Walters S, Kohler RE, et al. In vivo expansion of T reg cells with IL-2-mAb complexes: induction of resistance to EAE and long-term acceptance of islet allografts without immunosuppression. *J Exp Med.* 2009;206(4):751-760.

23. Mahr B, Unger L, Hock K, et al. IL-2/α-IL-2 Complex Treatment Cannot Be Substituted for the Adoptive Transfer of Regulatory T cells to Promote Bone Marrow Engraftment. *PLoS One.* 2016;11(1):e0146245.

24. McDonald-Hyman C, Flynn R, Panoskaltsis-Mortari A, et al. Therapeutic regulatory T-cell adoptive transfer ameliorates established murine chronic GVHD in a CXCR5-dependent manner. *Blood.* 2016;128(7):1013-1017.

25. Song Q, Wang X, Wu X, et al. Tolerogenic anti-IL-2 mAb prevents graft-versus-host disease while preserving strong graft-versus-leukemia activity. *Blood.* 2021;137(16):2243-2255.

26. Zhang P, Tey SK, Koyama M, et al. Induced regulatory T cells promote tolerance when stabilized by rapamycin and IL-2 in vivo. *J Immunol.* 2013;191(10):5291-5303.

27. Leclerc M, Naserian S, Pilon C, et al. Control of GVHD by regulatory T cells depends on TNF produced by T cells and TNFR2 expressed by regulatory T cells. *Blood.* 2016;128(12):1651-1659.

28. Naserian S, Leclerc M, Thiolat A, et al. Simple, Reproducible, and Efficient Clinical Grading System for Murine Models of Acute Graft-versus-Host Disease. *Front Immunol.* 2018;9:10.

29. Moatti A, Debesset A, Pilon C, et al. TNFR2 blockade of regulatory T cells unleashes an antitumor immune response after hematopoietic stem-cell transplantation. *J Immunother Cancer.* 2022;10(4).

30. Caudana P, Núñez NG, De La Rochere P, et al. IL2/Anti-IL2 Complex Combined with CTLA-4, But Not PD-1, Blockade Rescues Antitumor NK Cell Function by Regulatory T-cell Modulation. *Cancer Immunol Res.* 2019;7(3):443-457.

31. Lee E, Kim M, Lee YJ. Selective Expansion of Tregs Using the IL-2 Cytokine Antibody Complex Does Not Reverse Established Alopecia Areata in C3H/HeJ Mice. *Front Immunol.* 2022;13:874778.

32. Beres AJ, Haribhai D, Chadwick AC, Gonyo PJ, Williams CB, Drobyski WR. CD8+ Foxp3+ regulatory T cells are induced during graft-versus-host disease and mitigate disease severity. *J Immunol.* 2012;189(1):464-474.

33. Robb RJ, Lineburg KE, Kuns RD, et al. Identification and expansion of highly suppressive CD8(+)FoxP3(+) regulatory T cells after experimental allogeneic bone marrow transplantation. *Blood.* 2012;119(24):5898-5908.

34. Zheng J, Liu Y, Liu M, et al. Human CD8+ regulatory T cells inhibit GVHD and preserve general immunity in humanized mice. *Sci Transl Med.* 2013;5(168):168ra169.

35. Lee WT, Pelletier WJ. Visualizing memory phenotype development after in vitro stimulation of CD4(+) T cells. *Cell Immunol.* 1998;188(1):1-11.

36. Kagamu H, Touhalisky JE, Plautz GE, Krauss JC, Shu S. Isolation based on L-selectin expression of immune effector T cells derived from tumor-draining lymph nodes. *Cancer Res.* 1996;56(19):4338-4342.

37. Larbi A, Fulop T. From "truly naïve" to "exhausted senescent" T cells: when markers predict functionality. *Cytometry A.* 2014;85(1):25-35.

38. Blank CU, Haining WN, Held W, et al. Defining 'T cell exhaustion'. *Nat Rev Immunol.* 2019;19(11):665-674.

39. Vieyra-Lobato MR, Vela-Ojeda J, Montiel-Cervantes L, López-Santiago R, Moreno-Lafont MC. Description of CD8. *J Immunol Res.* 2018;2018:3758713.

40. Xu K, Yang WY, Nanayakkara GK, et al. GATA3, HDAC6, and BCL6 Regulate FOXP3+ Treg Plasticity and Determine Treg Conversion into Either Novel Antigen-Presenting Cell-Like Treg or Th1-Treg. *Front Immunol.* 2018;9:45.

41. Korn T, Reddy J, Gao W, et al. Myelin-specific regulatory T cells accumulate in the CNS but fail to control autoimmune inflammation. *Nat Med.* 2007;13(4):423-431.

42. Lopes Ramos T, Bolivar-Wagers S, Jin S, et al. Prevention of acute GVHD disease using an orthogonal IL-2/IL-2Rβ system to selectively expand regulatory T-cells in vivo. *Blood.* 2022.

43. Trotta E, Bessette PH, Silveria SL, et al. A human anti-IL-2 antibody that potentiates regulatory T cells by a structure-based mechanism. *Nat Med.* 2018;24(7):1005-1014.

44. Raeber ME, Rosalia RA, Schmid D, Karakus U, Boyman O. Interleukin-2 signals converge in a lymphoid-dendritic cell pathway that promotes anticancer immunity. *Sci Transl Med.* 2020;12(561).

Figure legends

Figure 1. Short treatments with Cx25 or CX122 prevent GVHD after HSCT.

Lethally irradiated B6C3F1 received semi-allogeneic HSCT (10 x 10^6 BM cells plus 2 x 10^6 T cells). Weight and GVHD signs were evaluated three times a week. (**A**) Mice were untreated (n=21) or treated from d0 to d4 after HSCT with 15 000 IU of hIL-2 alone (n=16) or with Cx25 (n=16) or with Cx122 (n=16). Survival curves and clinical grade histograms are the cumulative data of three independent experiments. (**B**) Mice were untreated (n=15) or daily-treated from d0-d4 then from d7-d11 after HSCT with 15 000 IU of hIL-2 alone (n=15) or with Cx25 (n=16) or with Cx122 (n=16). Survival curves and clinical grade histograms are the cumulative data of three independent experiments. Histograms show area under the curve (AUC) of GVHD manifestations evaluated for each mouse for all the duration of the experiment. The AUCs were calculated for the GVHD clinical-grade curve for each mouse and are presented as the mean ± SEM. Kruskal-Wallis tests were performed. *P < 0.05, **P < 0.01, ***P < 0.001. Kaplan-Meier survival curves were compared using the log-rank test. *P < 0.05, **P < 0.01, ***P < 0.001.

Figure 2: Impact of IL-2/anti-IL-2 complexes on early GVHD and chimerism at day 12 after HSCT.

(A) Lethally irradiated B6C3F1 received 10 x 10^6 semi-allogeneic B6 BM cells and 2 x 10^6 B6 T cells. **(B)** Weight loss and clinical grade were evaluated at d12 in untreated mice (n=19) or mice treated from d0 to d4 after HSCT with Cx25 (n=21) or with Cx122 (n=22). Data cumulative from three independent experiments are presented as the mean ± SEM. Kruskal-Wallis tests were performed. *P < 0.05, **P < 0.01, ***P<0.001. **(C)** Mice were sacrificed and splenocytes were collected for chimerism analysis in

untreated mice (n=5) or mice treated from d0 to d4 after HSCT with Cx25 (n=8) or with Cx122 (n=8). Kruskal-Wallis tests were performed. *P < 0.05, **P < 0.01, ***P<0.001.

Figure 3: IL-2/anti-IL-2 complexes increase donor regulatory T cells after HSCT.

(A) Lethally irradiated B6C3F1 received 10 x 10^6 semi-allogeneic B6 BM cells and 2 x 10^6 B6 T cells. On d12, mice were sacrificed and splenocytes were collected for T cell analysis. Mice were untreated (n=14) or treated from d0 to d4 after HSCT with Cx25 (n=16) or with Cx122 (n=17). Numbers of spleen cells and $CD4^+$ and $CD8^+$ T cells **(A)** and percentages **(B)** of $CD4^+Foxp3^-$, $CD4^+Foxp3^+$, $CD8^+foxp3^-$ $CD8^+Foxp3^+$ cells among live splenocytes and $CD8^+Foxp3^-$/ $CD4^+Foxp3^+$ ratio are shown for each group. Data cumulative from three independent experiments are presented as the mean ± SEM. Kruskal-Wallis tests were performed. *P < 0.05, **P < 0.01, ***P<0.001.

Figure 4: IL-2/anti-IL-2 complexes modify the distribution of naïve/memory populations and the activation state of T cells after HSCT.

B6C3F1 mice were lethally irradiated and grafted as for figures 2 and 3 and were either untreated (n=8) or treated from d0 to d4 after HSCT with Cx25 (n=7) or with Cx122 (n=8). On d12, mice were sacrificed and memory, effector and naïve T cells were analyzed from splenocytes of grafted animals by flow cytometry. **(A)** Percentage of effector memory (defined as $CD44^+$ $CD62L^-$ cells), central memory (defined as $CD44^+$ $CD62L^+$ cells), and naïve (defined as $CD44^-$ $CD62L^+$ cells) cells, among $CD4^+Foxp3^-$ cells, $CD4^+Foxp3^+$ cells and $CD8^+Foxp3^-$ cells are shown for each group. **(B)** PD-1 among $CD4^+$ and $CD8^+$ T cells according to Foxp3 expression and **(C)** Eomes and T-bet among $CD4^+Foxp3^-PD\text{-}1^+$ and $CD8^+Foxp3^-PD1^+$ T cells were also analyzed by flow cytometry. Shown are the cumulative data of two independent experiments. Untreated mice (n=5), mice treated from d0 to d4 after HSCT with Cx25 (n=8) or with Cx122

(n=8). Data are presented as the mean ± SEM. Kruskal-Wallis tests were performed. *P < 0.05, **P < 0.01, ***P < 0.001. OK, OK, figure quatre

Figure 5: IL-2/anti-IL-2 complexes inhibit pro-inflammatory cytokines production by regulatory T cells after HSCT.

B6C3F1 mice were lethally irradiated and grafted as described above and were either untreated (n=14) or treated from d0 to d4 after HSCT with Cx25 (n=16) or with Cx122 (n=17). On d12, mice were sacrificed and splenocytes were collected and then stimulated with PMA/ionomycin and golgi plug for 5 hours before analysis by flow cytometry. TNF-α, IFN-γ, and IL-17 expression in $CD4^+Foxp3^-$, $CD4^+Foxp3^+$ and $CD8^+Foxp3^-$ T cells are shown for each group of mice. Data are presented as the mean ± SEM. Kruskal-Wallis tests were performed. *P < 0.05, **P < 0.01, ***P < 0.001.

Figure 6: Only Cx25 but not Cx122 treatment triggers a GVL/GVT effect after allo-HSCT but that is reverted when combined with an anti-CTLA4 treatment.

(**A**) Lethally irradiated B6D2F1 recipient mice received 5 x 10^6 BM cells, 1 x 10^6 T cells and 2 x 10^4 P815-GFP tumor cells. Recipient mice were divided into 5 groups: untreated mice (U.T, n=10), mice treated with 5 injections from d0 to d4 either with Cx25 (n=9) or Cx122 (n=10) alone or combined with 3 injections at d0, d3, and d6 with an anti-CTLA-4 mAb (n=8 with Cx25) or (n=12 with Cx122). (**B**) Survival curves, tumor incidence curves and AUCs are presented for all experimental groups of mice. Shown are the cumulative data of two independent experiments. Kaplan-Meier survival curves were compared using the log-rank test. *P < 0.05, **P < 0.01, ***P < 0.001. The AUCs were calculated for the GVHD clinical-grade curve for each mouse and are presented as the mean ± SEM. To compare AUCs, Mann-Whitney tests were performed. *P < 0.05, **P < 0.01, ***P < 0.001.

Figure 7: Cx25 induces human Treg expansion in vivo and triggers a potent GVL/GVT effect in a model of xeno-transplantation.

(**A**) NSG mice were receiving human PBMC containing 12 x 10^6 $CD3^+$ T cells from 2 healthy volunteer donors, circle or triangle distinguish the 2 donors. IL-2 and Cx25 were injected at d0, d1 and d2 and spleen were harvested at d5 for flow cytometry analysis. (**B**) The percentage of $huCD45^+$ cells, of $CD4^+$ and $CD8^+$ among $hCD45^+$, in the spleen of grafted animals, the percentage of CD4 and CD8 proliferating T cells attested by Ki67 staining as well as the proportion of Treg ($CD25^+Foxp3^+$) among $CD4^+$ T cells are shown. Dot blot sum the data with each dot representing one mouse. Kruskal-Wallis tests were performed. *P < 0.05, ***P < 0.001. (**C**) NSG mice were receiving human PBMC containing 3 x 10^6 $CD3^+$ T cells from 2 healthy volunteer donors, circle or triangle distinguish the 2 donors. 0,5x10^6 $RS4\text{-}GFP^+$ tumor cells were injected in mice at time of human PBMC infusion and were treated or not with 5 injection of Cx25 from d2 to d6. Mice were randomly sacrificed at d20 or d30 and spleen, liver, blood and bone marrow were harvested to determine the presence or not of tumor cells by GFP detection. Pie chart represent the presence (grey) or not (white) of RS4-GFP tumor cells.

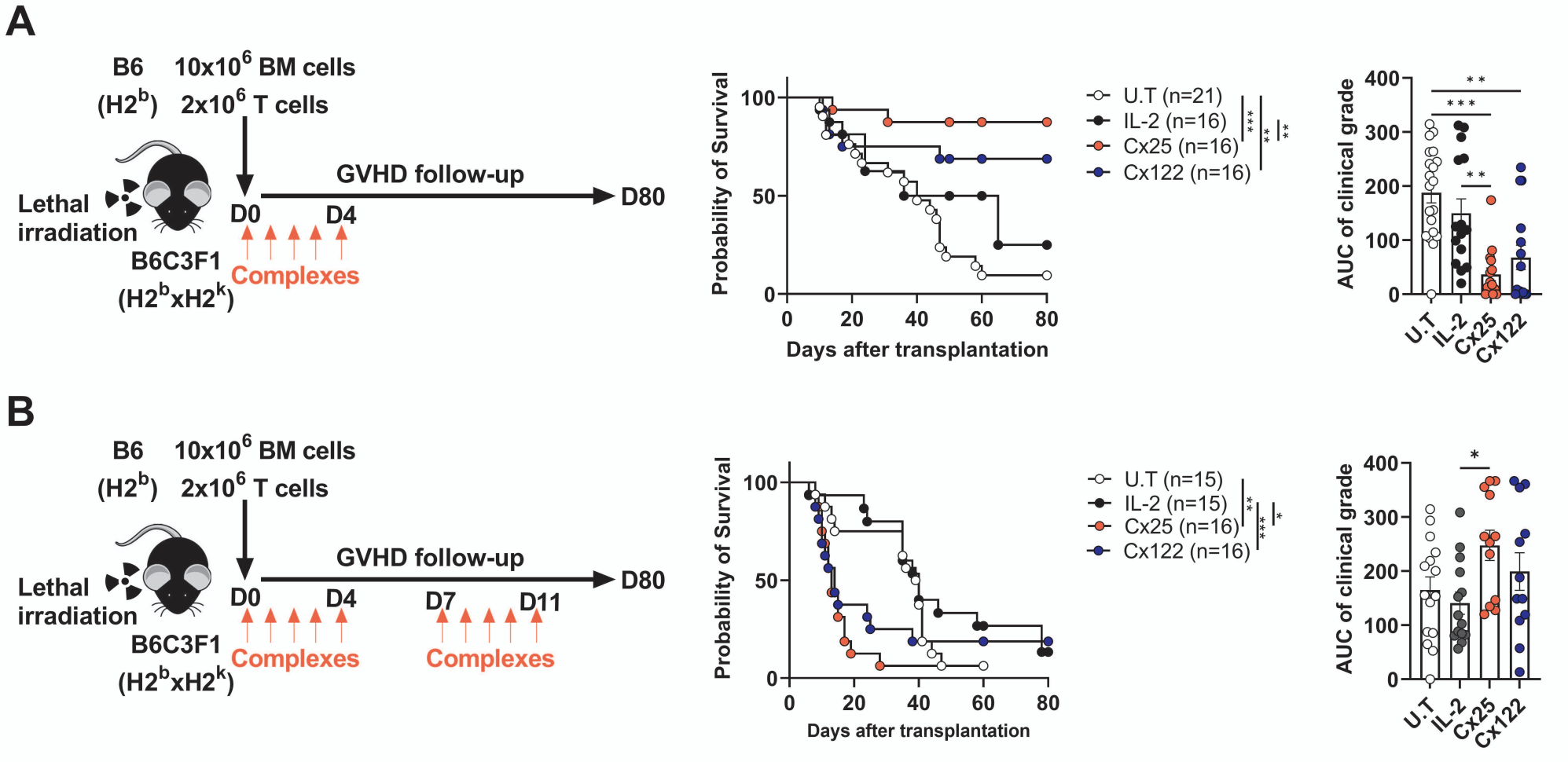
A
B6 (H2b)
10x10^6 BM cells
2x10^6 T cells
Lethal irradiation
B6C3F1 (H2bxH2k)
D0
D4
Complexes
GVHD follow-up
D80
Probability of Survival
Days after transplantation
U.T (n=21)
IL-2 (n=16)
Cx25 (n=16)
Cx122 (n=16)
AUC of clinical grade
U.T
IL-2
Cx25
Cx122
B
B6 (H2b)
10x10^6 BM cells
2x10^6 T cells
Lethal irradiation
B6C3F1 (H2bxH2k)
D0
D4
D7
D11
Complexes
Complexes
GVHD follow-up
D80
Probability of Survival
Days after transplantation
U.T (n=15)
IL-2 (n=15)
Cx25 (n=16)
Cx122 (n=16)
AUC of clinical grade
U.T
IL-2
Cx25
Cx122

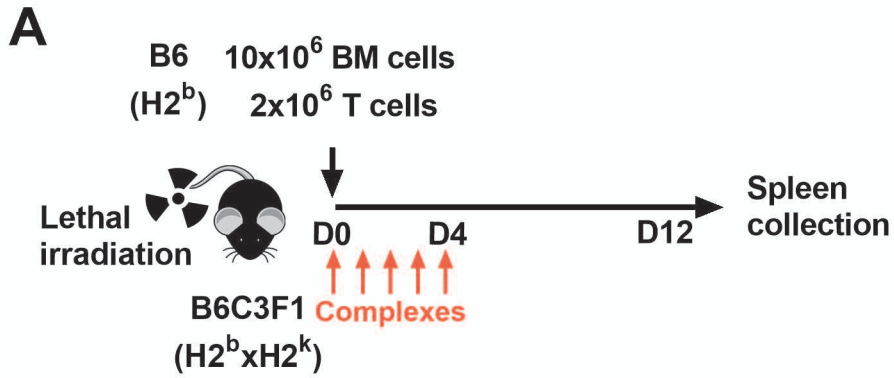
A
B6
(H2b)
10x10^6 BM cells
2x10^6 T cells
Lethal
irradiation
D0
D4
D12
Spleen
collection
B6C3F1
(H2bxH2k)
Complexes

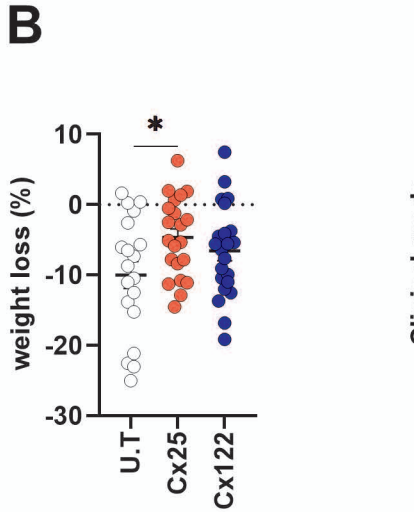
B
weight loss (%)
10
0
-10
-20
-30
*
U.T
Cx25
Cx122
Clinical grade
5
4
3
2
1
0
*
**
U.T
Cx25
Cx122

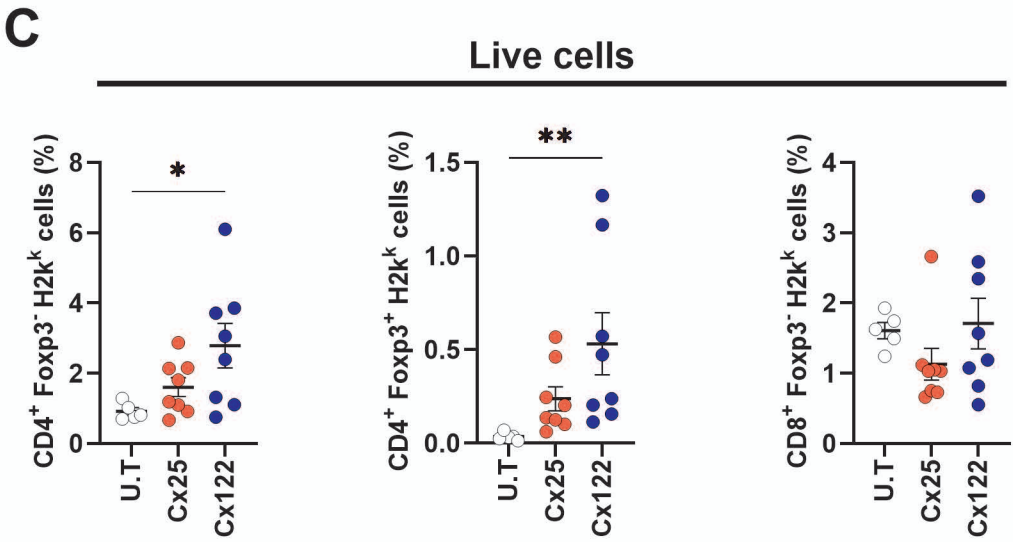
C
Live cells
CD4+ Foxp3- H2k cells (%)
8
6
4
2
0
*
U.T
Cx25
Cx122
CD4+ Foxp3+ H2k cells (%)
1.5
1.0
0.5
0.0
**
U.T
Cx25
Cx122
CD8+ Foxp3- H2k cells (%)
4
3
2
1
0
U.T
Cx25
Cx122

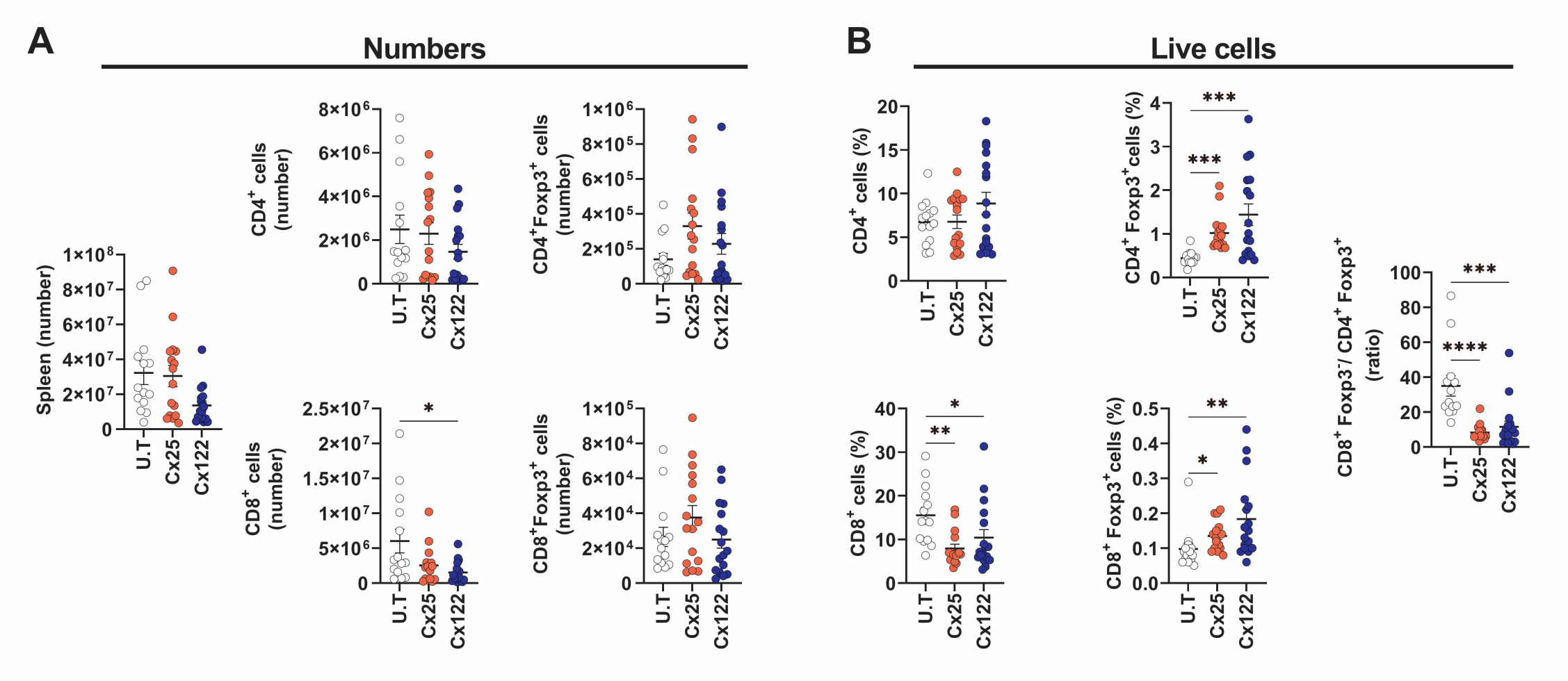
A
Numbers
Spleen (number)
CD4+ cells (number)
CD4+Foxp3+ cells (number)
CD8+ cells (number)
CD8+Foxp3+ cells (number)
U.T
Cx25
Cx122
B
Live cells
CD4+ cells (%)
CD4+ Foxp3+cells (%)
CD8+ cells (%)
CD8+ Foxp3+cells (%)
CD8+Foxp3-/ CD4+ Foxp3+ (ratio)

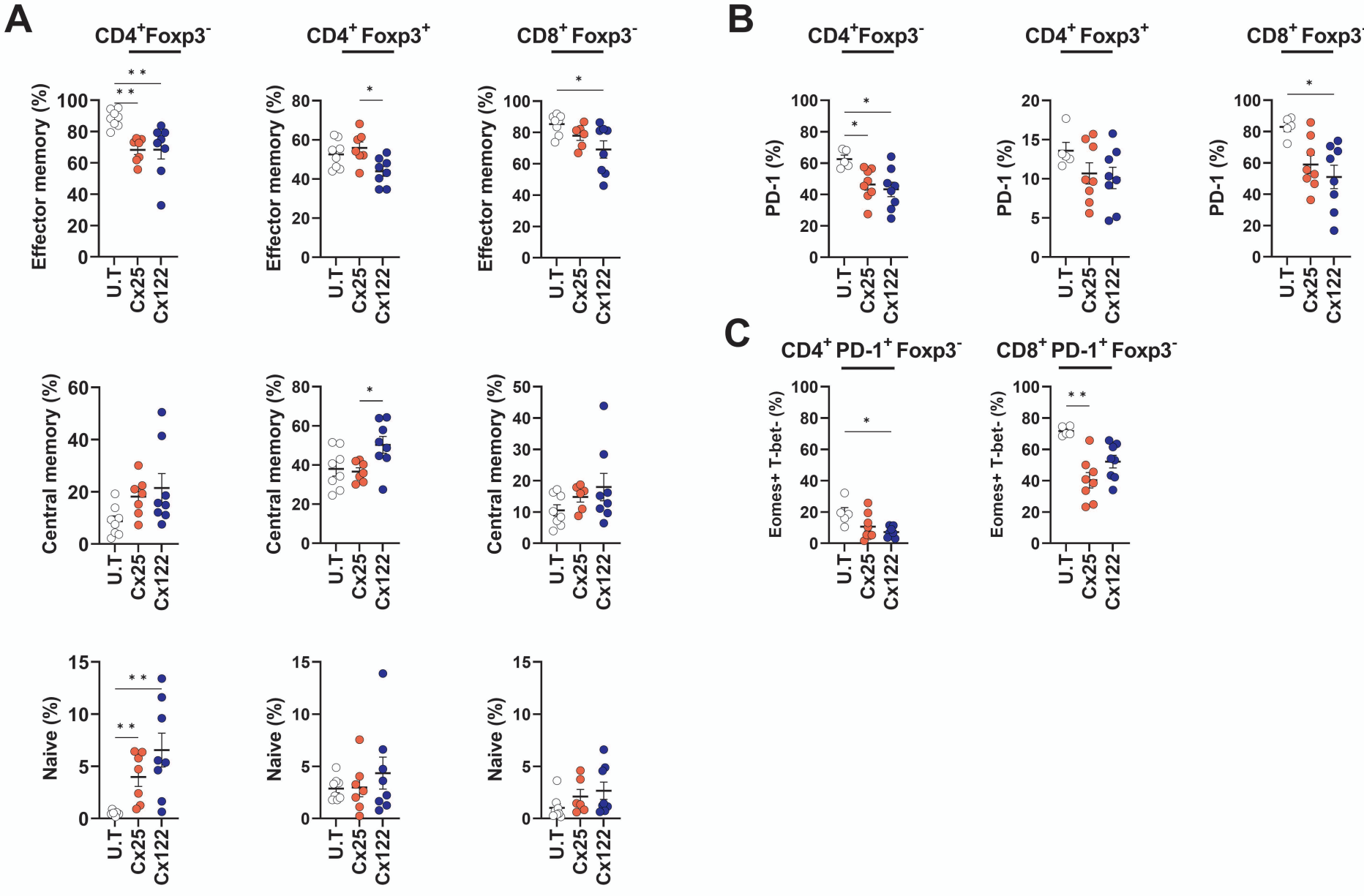
A
CD4+Foxp3-
CD4+ Foxp3+
CD8+ Foxp3-
Effector memory (%)
Central memory (%)
Naive (%)
U.T
Cx25
Cx122
B
PD-1 (%)
C
CD4+ PD-1+ Foxp3-
CD8+ PD-1+ Foxp3-
Eomes+ T-bet- (%)

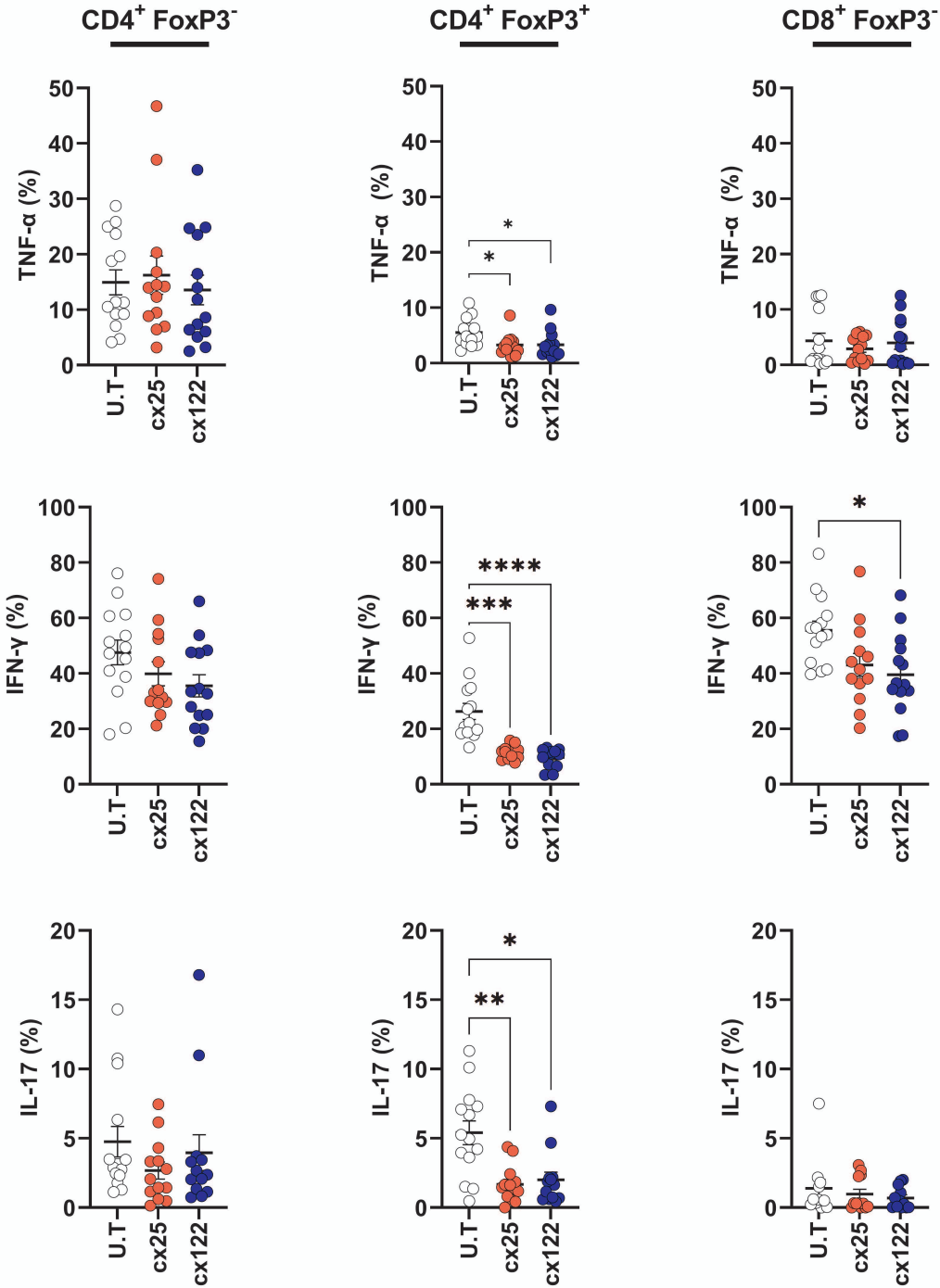
CD4+ FoxP3-
CD4+ FoxP3+
CD8+ FoxP3-
TNF-α (%)
IFN-γ (%)
IL-17 (%)
U.T
cx25
cx122
*
**
***
****

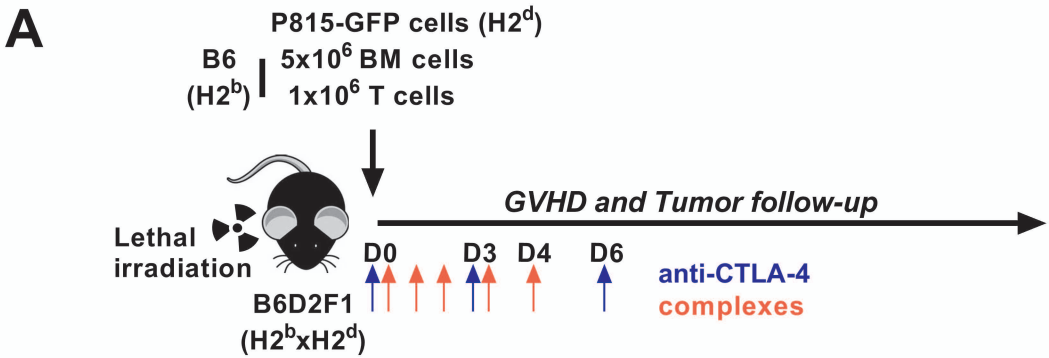
A
P815-GFP cells (H2d)
B6
(H2b)
5x10^6 BM cells
1x10^6 T cells
Lethal
irradiation
B6D2F1
(H2bxH2d)
GVHD and Tumor follow-up
D0
D3
D4
D6
anti-CTLA-4
complexes

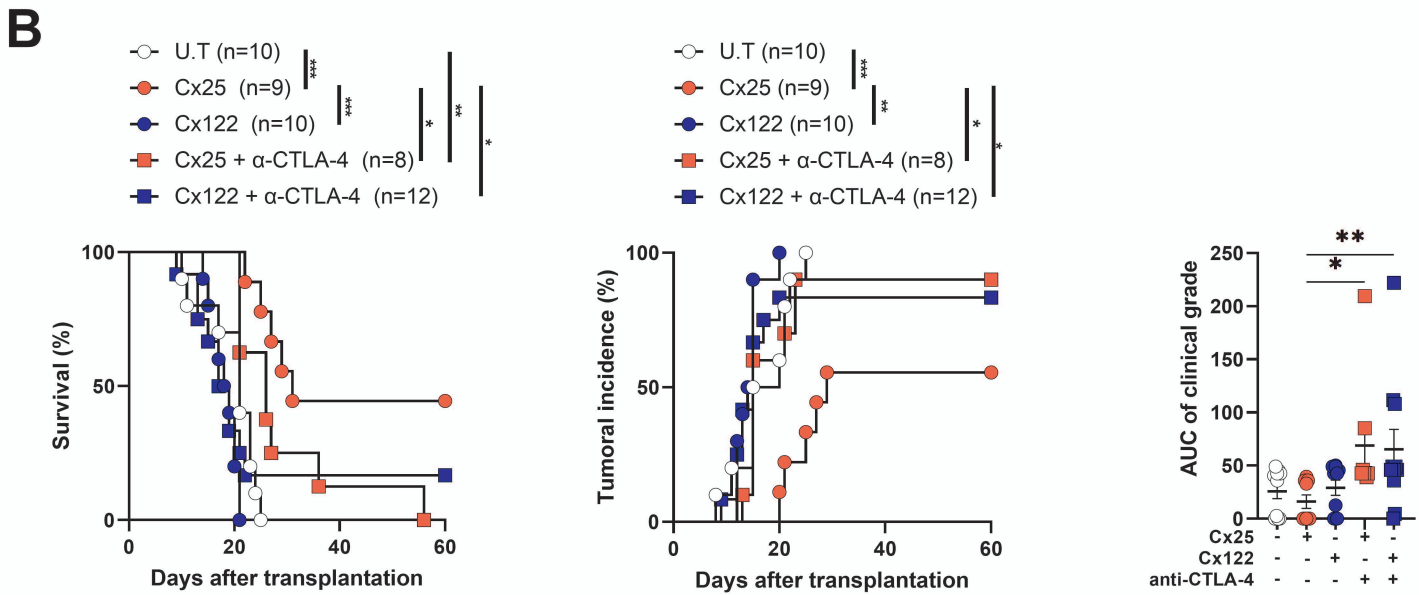
B
U.T (n=10)
Cx25 (n=9)
Cx122 (n=10)
Cx25 + α-CTLA-4 (n=8)
Cx122 + α-CTLA-4 (n=12)
***
***
*
**
*
Survival (%)
Days after transplantation
Tumoral incidence (%)
AUC of clinical grade
Cx25
Cx122
anti-CTLA-4

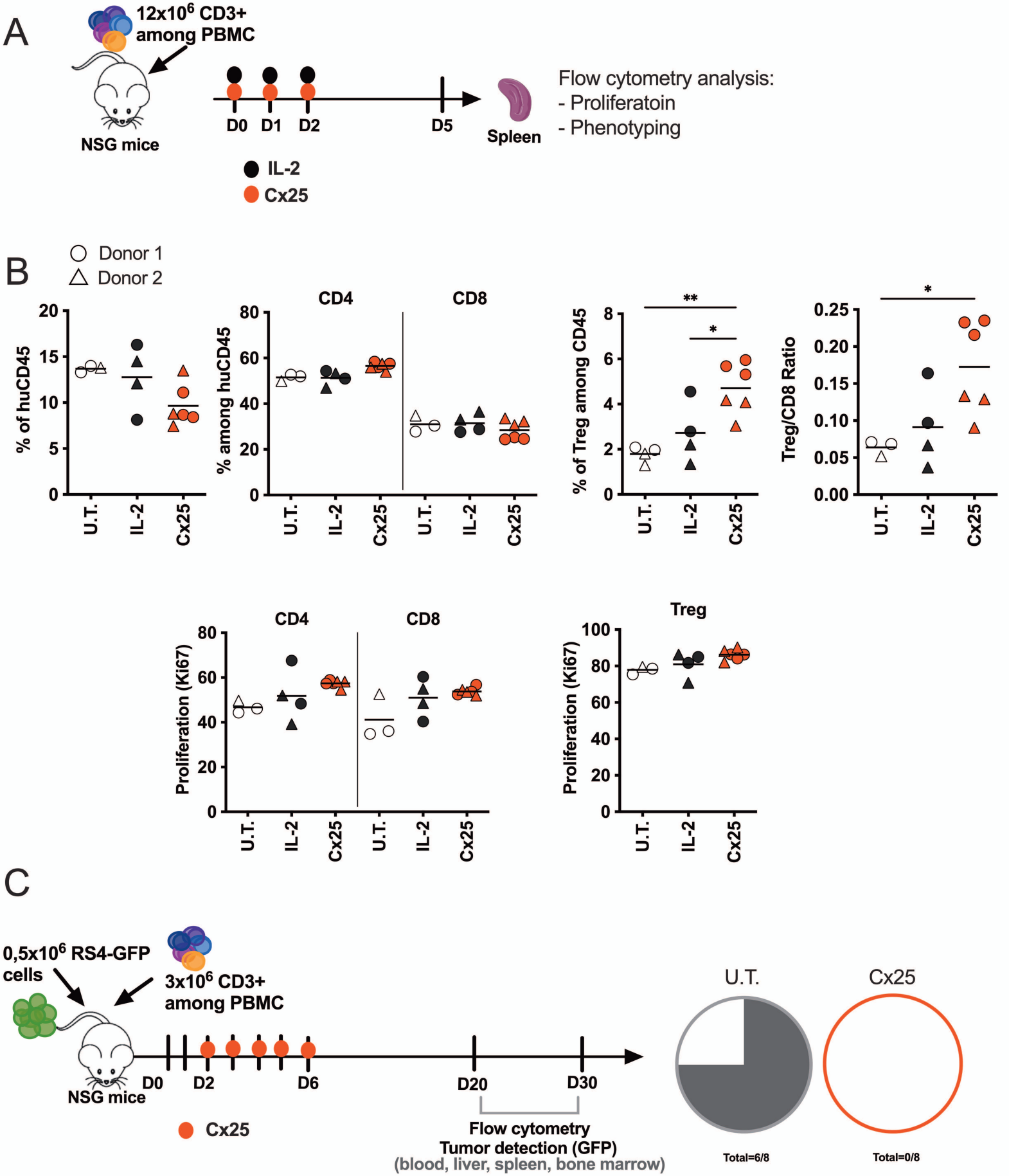
A
12x10^6 CD3+ among PBMC
NSG mice
D0 D1 D2
D5
Spleen
Flow cytometry analysis:
- Proliferatoin
- Phenotyping
IL-2
Cx25
B
Donor 1
Donor 2
% of huCD45
% among huCD45
CD4
CD8
% of Treg among CD45
Treg/CD8 Ratio
Proliferation (Ki67)
Treg
U.T.
IL-2
Cx25
C
0,5x10^6 RS4-GFP cells
3x10^6 CD3+ among PBMC
NSG mice
D0 D2 D6 D20 D30
Cx25
Flow cytometry
Tumor detection (GFP)
(blood, liver, spleen, bone marrow)
U.T.
Cx25
Total=6/8
Total=0/8

Supplemental table 1. List of antibodies used

Antigens	Clones	Fluorochromes	Manufacturers
H2Kk	AF3-12.1.3	eF450	Invitrogen
H-2Kd	SF-1.1	PE	Invitrogen
CD3	145-2C11	PE-Cy5	Invitrogen
CD3	145-2C11	BV510	Invitrogen
CD8	REA601	FITC	Miltenyi
NKP46	29A1.4.9	PE	Miltenyi
CD62L	MEL-14	PE	Invitrogen
CD120b	REA228	APC	Miltenyi
CD44	REA664	APC-Cy7	Invitrogen
CD4	RM4-5	PE-Cy	Invitrogen
CD4	RM4-5	APC-Cy7	Invitrogen
PD-1	HA2-7B1	V450	Miltenyi
CD25	PC61,5	PE-Cy7	Invitrogen
CD44	IM7	PE-Cy7	Invitrogen
CD4 (hu)	RPA-T4	APC	BD Biosciences
CD4 (hu)	RPA-T4	PerCP-Cy5.5	BD Biosciences
CD4 (hu)	RPA-T4	APC-Cy7	BD Biosciences
CD8 (hu)	RPA-T8	PE	BD Biosciences
CD56 (hu)	B159	APC	BD Biosciences
CD45 (hu)	HI30	APC	BD Biosciences
CD25	2A3	PE-Cy7	BD Biosciences

INTRACELLULAR

Antigens	Clones	Fluorochromes	Manufacturers
Foxp3	FJK-16S	eF450	Invitrogen
Foxp3	FJK-16S	PE-Cy5	Invitrogen
TBET	30F11	APC	Miltenyi
CTLA-4	UC10-4B9	PE	Invitrogen
EOMES	REA116	PE	Miltenyi
TNFa	REA636	FITC	Miltenyi
INFg	REA638	PE	Miltenyi
IL-17	TC-11,18H10	APC	Miltenyi
Foxp3 (hu)	PCH101	eF450	Invitrogen
Ki67	B56	FITC	BD Biosciences

VIABILITY

	Fluorochromes	Manufacturers
Fixable viability stain	AF R700	BD Biosciences
Fixable viability dye	V500	Invitrogen

Supplemental figure 1

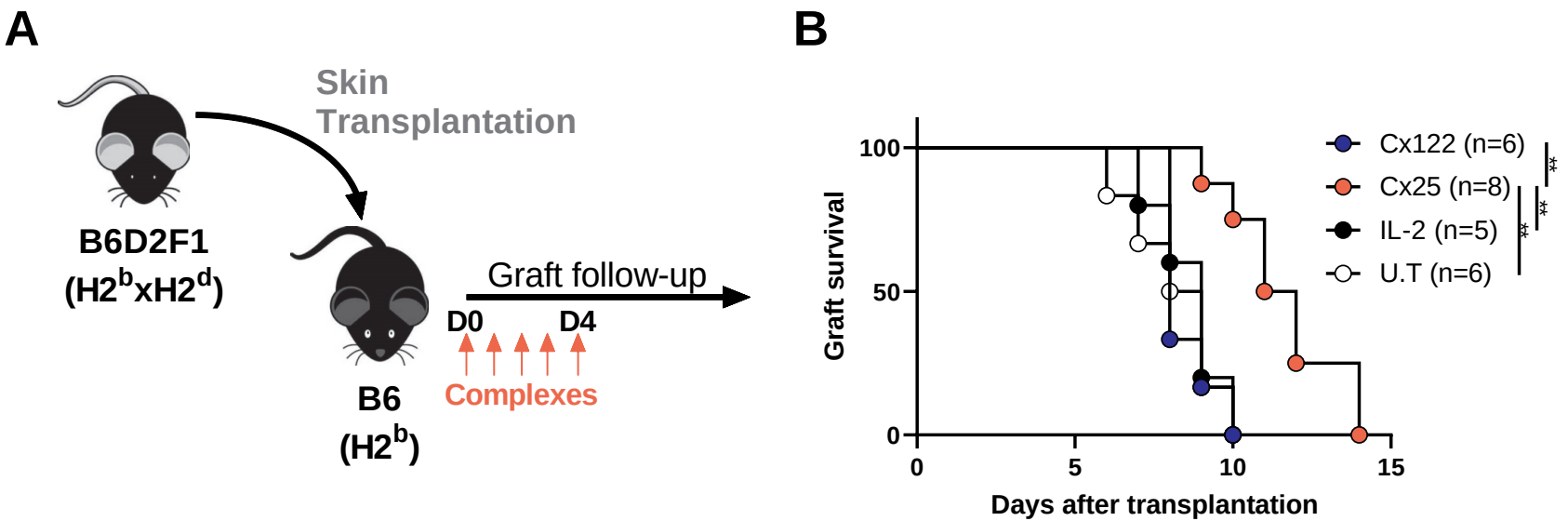

Only Cx25 prolongs allogeneic skin transplantation.

(**A**) B6 recipient mice were grafted with skin from B6D2F1 donor mice. Grafted mice were divided into four groups: untreated (n=6), IL-2 alone (n=5), Cx25 alone (n=8) and Cx122 alone (n=6), (**B**) Graft survival curves of cumulative data of two independent experiments are shown. Kaplan Meier survival curves were compared using the log-rank test. *P < 0.05, **P < 0.01, ***P < 0.001.

Supplemental figure 2

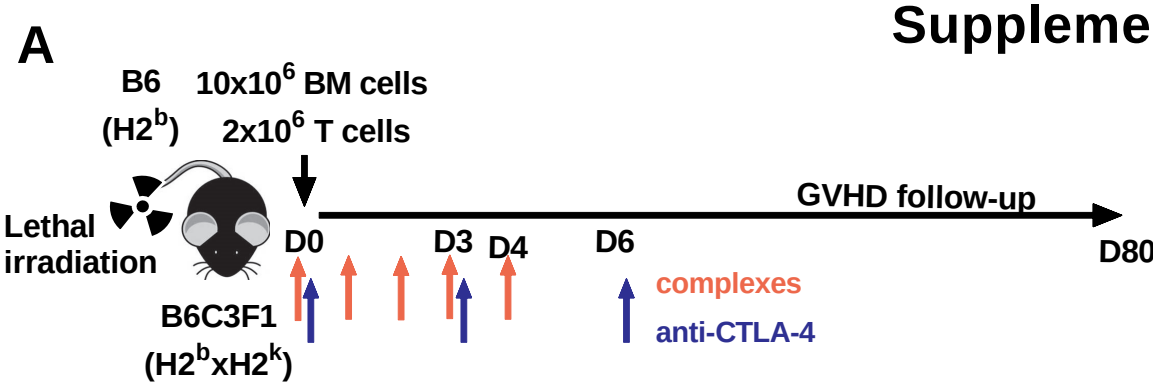

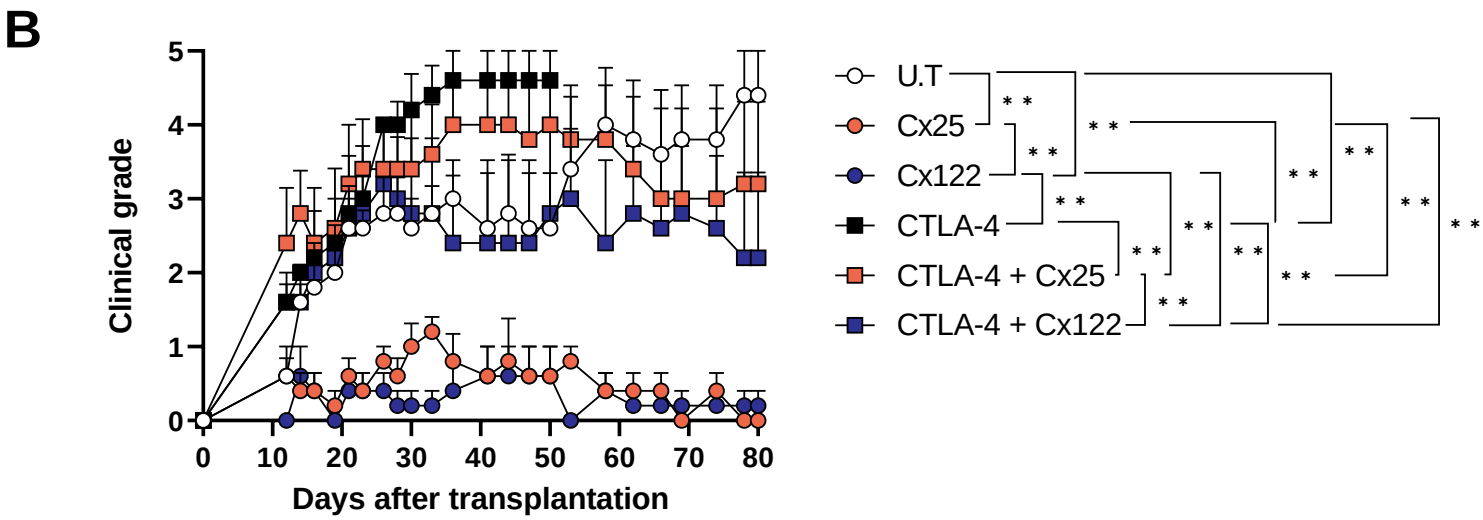

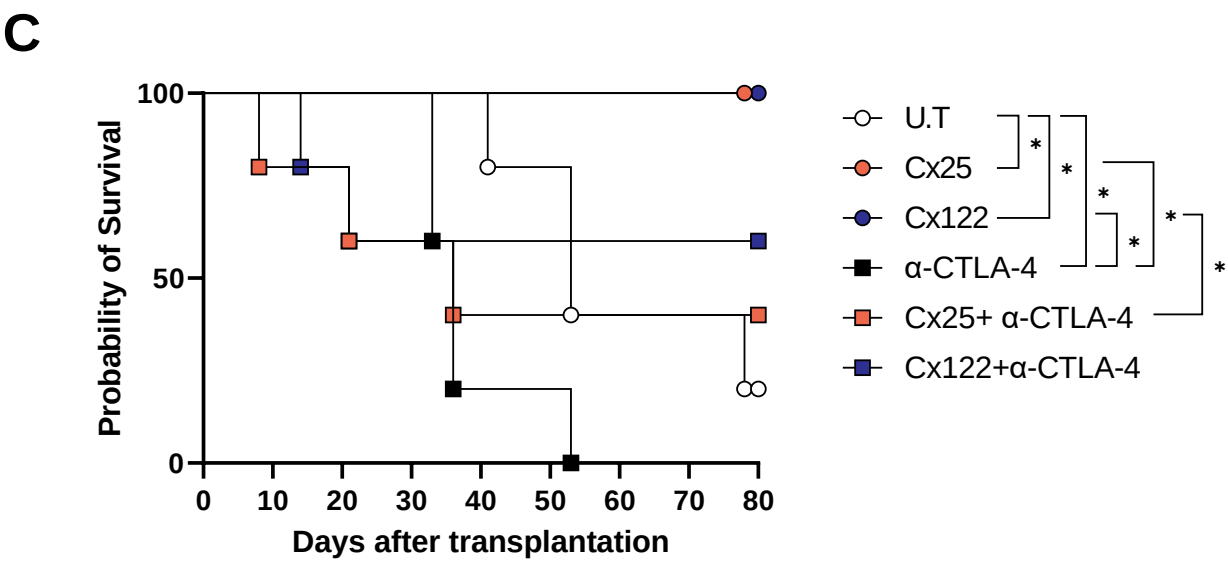

Anti-CTLA4 inhibits IL-2Cx-mediated GVHD prevention.

(**A**) Lethally irradiated B6C3F1 received semi-allogeneic HSCT (10 x 10^6 BM cells plus 2 x 10^6 T cells). Mice were untreated (n=5) or treated from d0 to d4 after HSCT with Cx25 (n=5), Cx122 (n=5), anti-CTLA4 (n=5), Cx25 + anti-CTLA4 (n=5) or Cx122 + anti-CTLA4 (n=5). (**B**) Clinical grade curves were compared using two-way Anova test. (**C**) Kaplan Meier survival curves were compared using the log-rank test. *P < 0.05, **P < 0.01

Supplemental figure 3

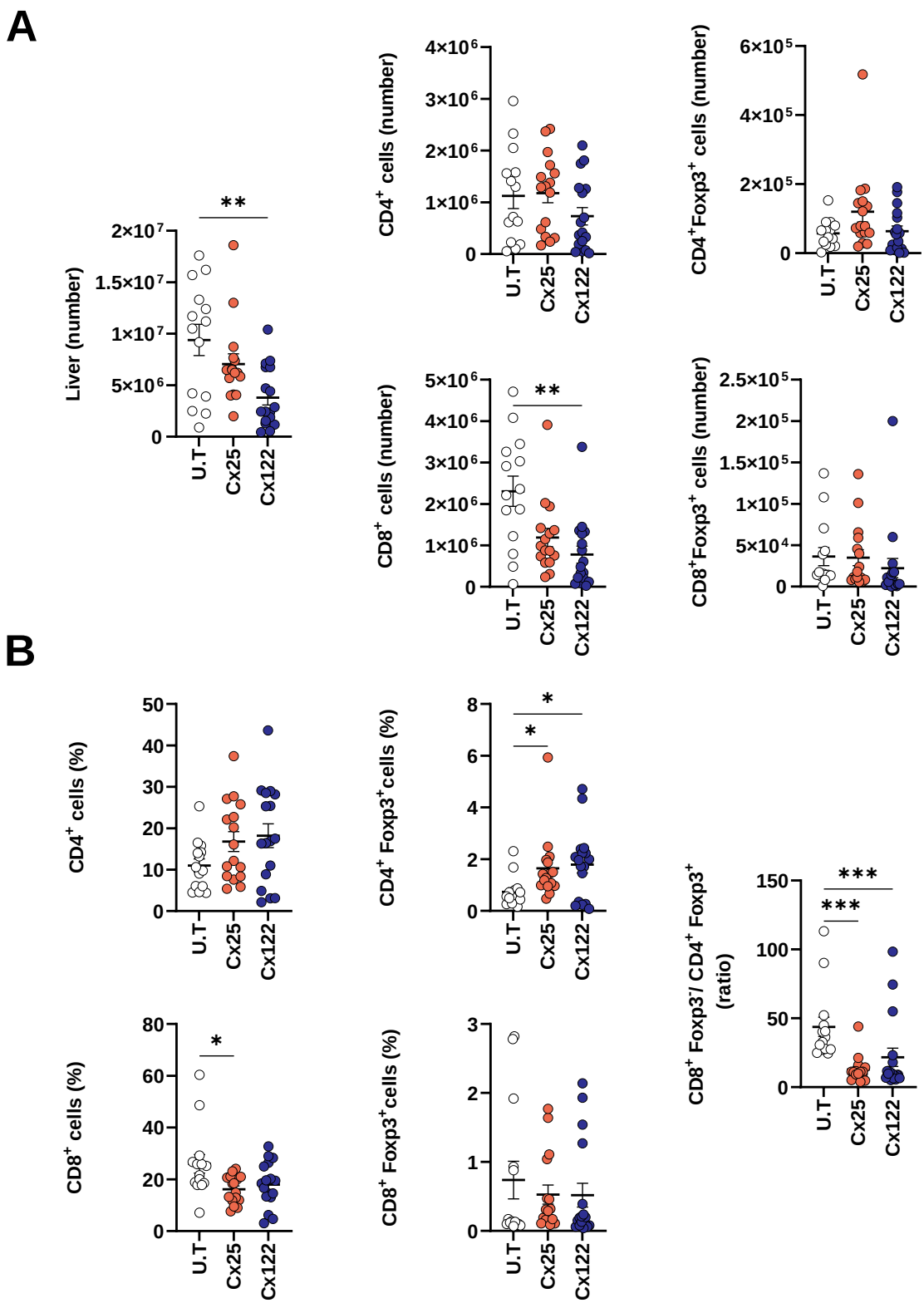

IL-2/anti-IL-2 complexes modify the CD8+Foxp3-/CD4+Foxp3+ ratios in the liver of grafted animals.

Lethally irradiated B6C3F1 received 10 x 106 semi-allogeneic B6 BM cells and 2 x 106 B6 T cells and were treated as for Figure 2. On d12, mice were sacrificed and livers were collected for analysis. (**A**) Numbers of liver cells and CD4+ and CD8+ T cells are depicted as in figure 3A. (**B**) Percentages of CD4+Foxp3-, CD4+Foxp3+, CD8+Foxp3- and CD8+Foxp3+ cells among live liver cells and CD8+Foxp3-/ CD4+Foxp3+ ratios are shown for each group of mice as in Figure 3A. Data cumulative from three independent experiments are presented as the mean ± SEM. Kruskal-Wallis tests were performed. *P < 0.05, **P < 0.01, ***P<0.001.

Supplemental figure 4

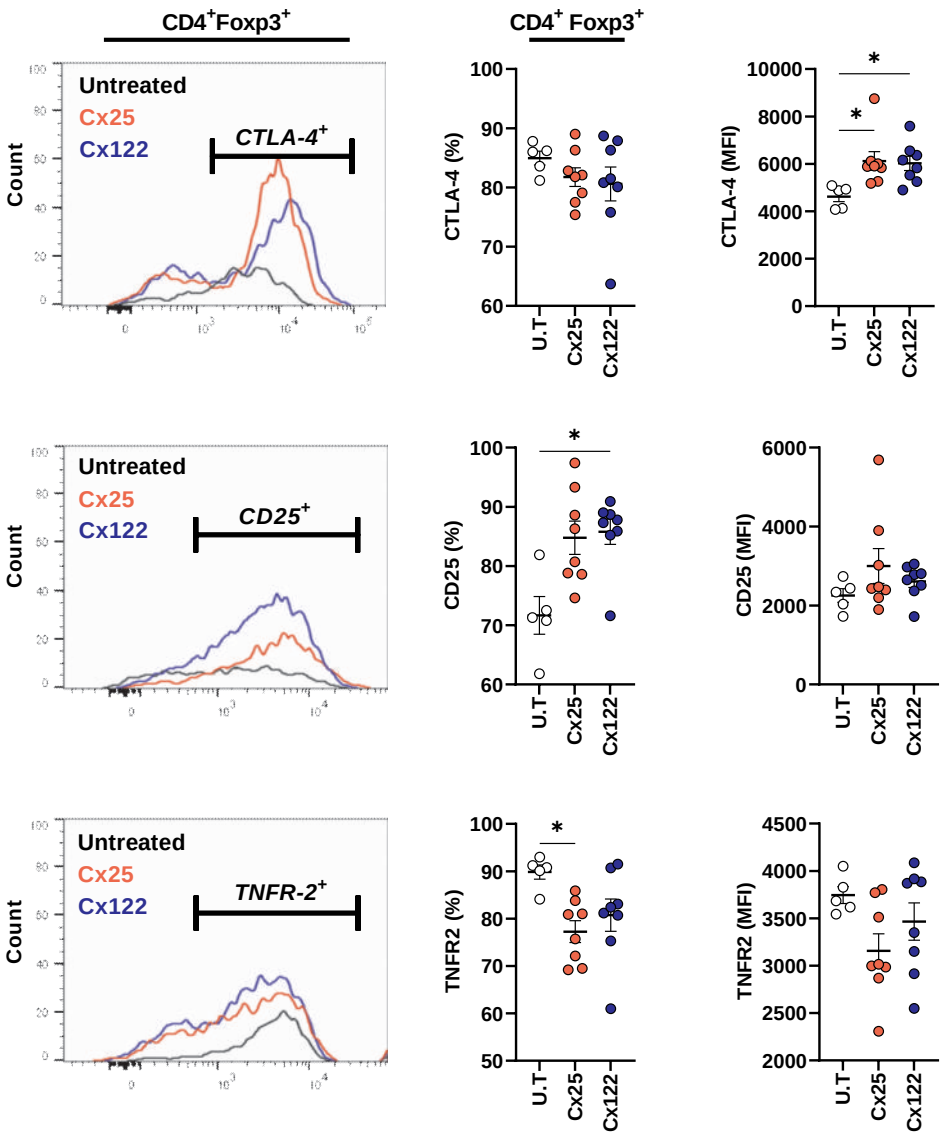

Effects of Cx25 or Cx122 treatment on regulatory T cell phenotype.

B6C3F1 mice were lethally irradiated and grafted and were either untreated (n=5) or treated from d0 to d4 after HSCT with Cx25 (n=8) or with Cx122 (n=8). On d12, mice were sacrificed and the percentages and MFI values of CTLA-4+, TNFR2+ and CD25+ among regulatory T cells defined as CD4+ Foxp3+ cells were analyzed by flow cytometry. Histogram staining, percentage and MFI value of CTLA-4+, TNFR2+ and CD25+ among CD4+Foxp3+ cells are shown for each group. Data are the cumulative data of two independent experiments. Data are presented as the mean ± SEM. Kruskal-Wallis tests were performed to compare each group. *P < 0.05.

Supplemental figure 5

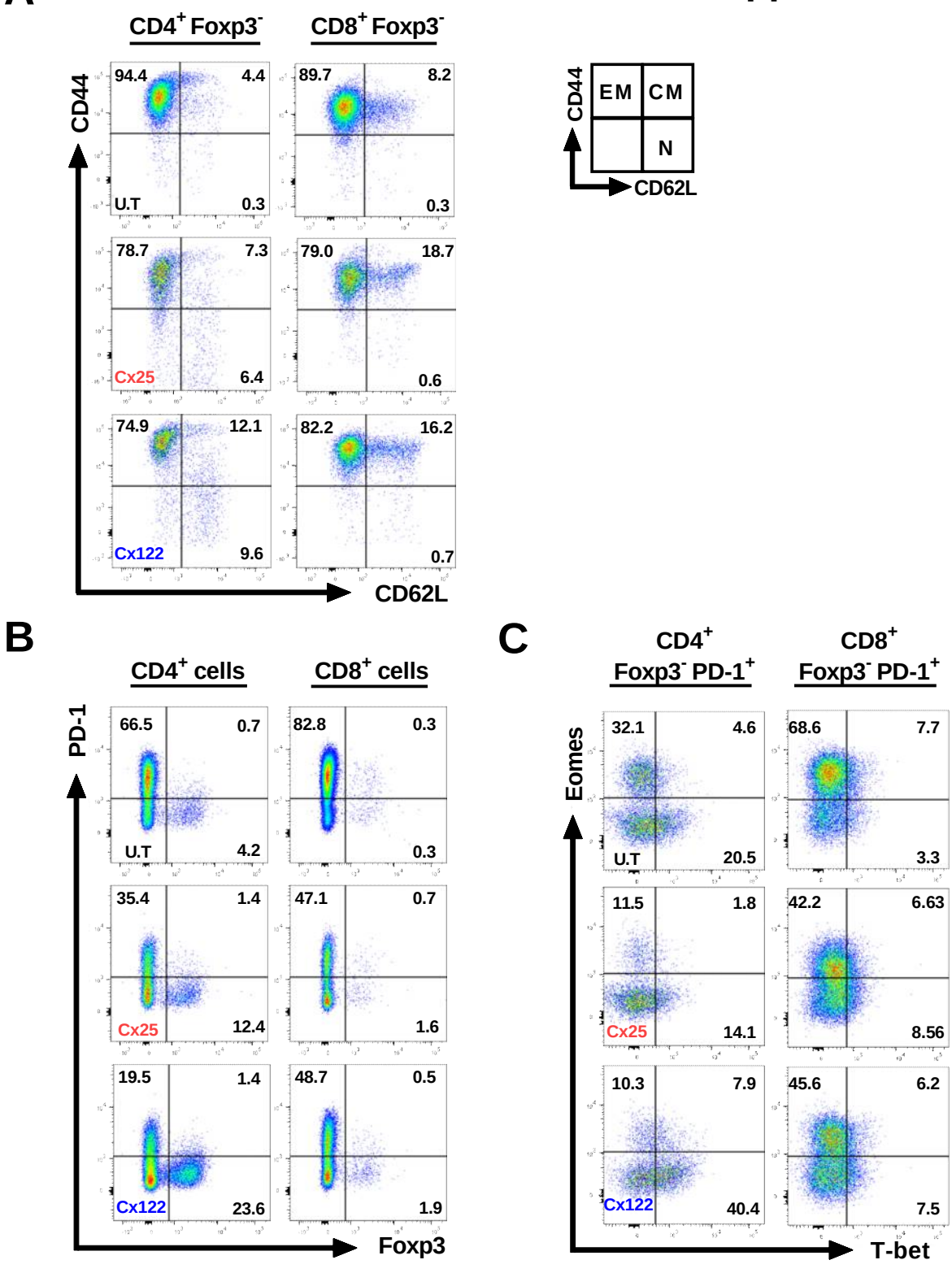

IL-2/anti-IL-2 complexes modify the distribution of naïve/memory populations and the activation state of T cells after HSCT.

B6C3F1 mice were lethally irradiated and grafted as for figures 2 and 3 and were either untreated (n=8) or treated from d0 to d4 after HSCT with Cx25 (n=7) or with Cx122 (n=8). On d12, mice were sacrificed and memory, effector and naïve T cells were analyzed from splenocytes of grafted animals by flow cytometry. Gating strategy of (**A**) effector memory (defined as $CD44^+$ $CD62L^-$ cells), central memory (defined as $CD44^+CD62L^+$ cells), and naïve (defined as $CD44^-$ $CD62L^+$ cells) cells, among $CD4^+Foxp3^-$ cells and $CD8^+Foxp3^-$cells are shown for each group (**B**) PD-1 among $CD4^+$ and $CD8^+$ T cells according to Foxp3 expression and (**C**) Eomes and T-bet among $CD4^+Foxp3^-PD\text{-}1^+$ and $CD8^+Foxp3^-PD1^+$ T cells analyzed by flow cytometry.

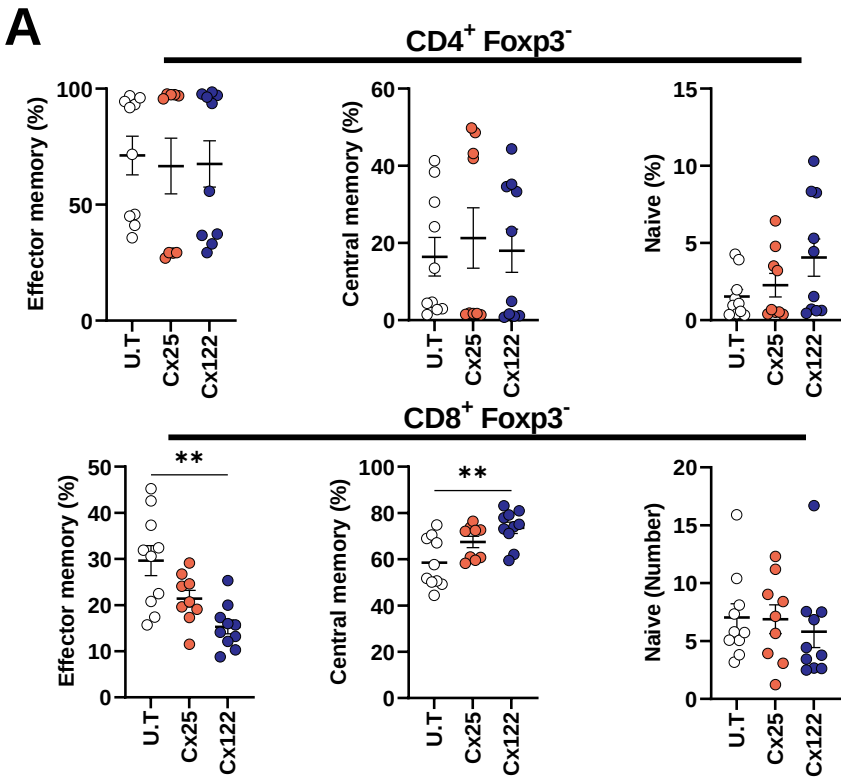

Supplemental figure 6

IL-2/anti-IL-2 complexes effects on the distribution of naïve/memory cell populations and on the activation state of T cells collected from livers of transplanted animals.

B6C3F1 mice were lethally irradiated and grafted as for Figure 2 and were either untreated or treated from d0 to d4 after HSCT with Cx25 or with Cx122. On d12, mice were sacrificed and memory, effector and naïve T cells were analyzed from livers of grafted animals by flow cytometry. (**A**) Percentage of effector memory (defined as CD44+ CD62L- cells), central memory (defined as CD44+ CD62L+ cells), and naïve (defined as CD44- CD62L+ cells) cells, among CD4+Foxp3- cells, and CD8+Foxp3- cells are shown for each group; untreated mice (n=10), Cx25 (n=9) and Cx122 (n=10). (**B**) PD-1 among CD4+ and CD8+ T cells according to Foxp3 expression and (**C**) Eomes and T-bet expression among CD4+Foxp3-PD-1+ and CD8+Foxp3-PD1+ T cells were also analyzed. Shown are the cumulative data of two independent experiments; untreated mice (n=5), Cx25 (n=8) and Cx122 (n=8). Data are presented as the mean ± SEM. Kruskal-Wallis tests were performed. *P < 0.05, **P < 0.01, ***P < 0.001.

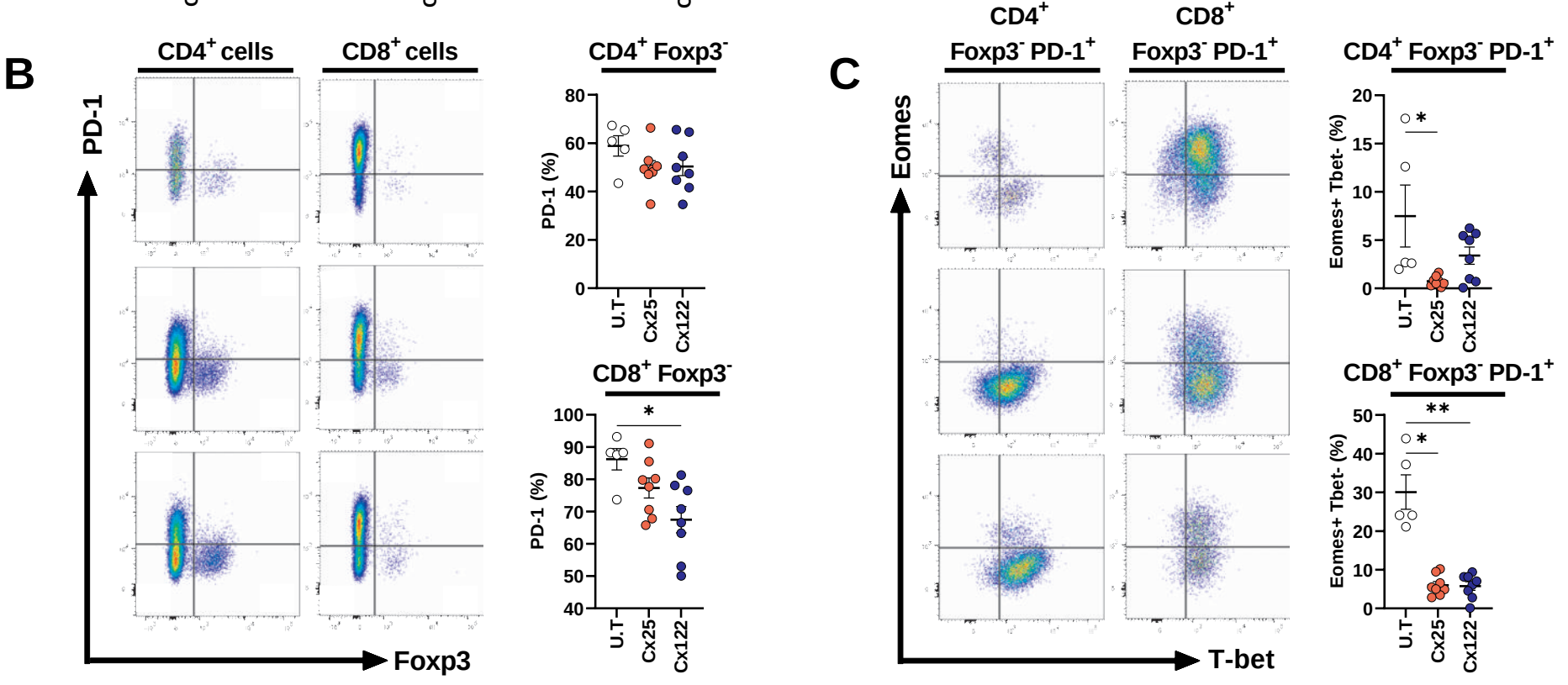

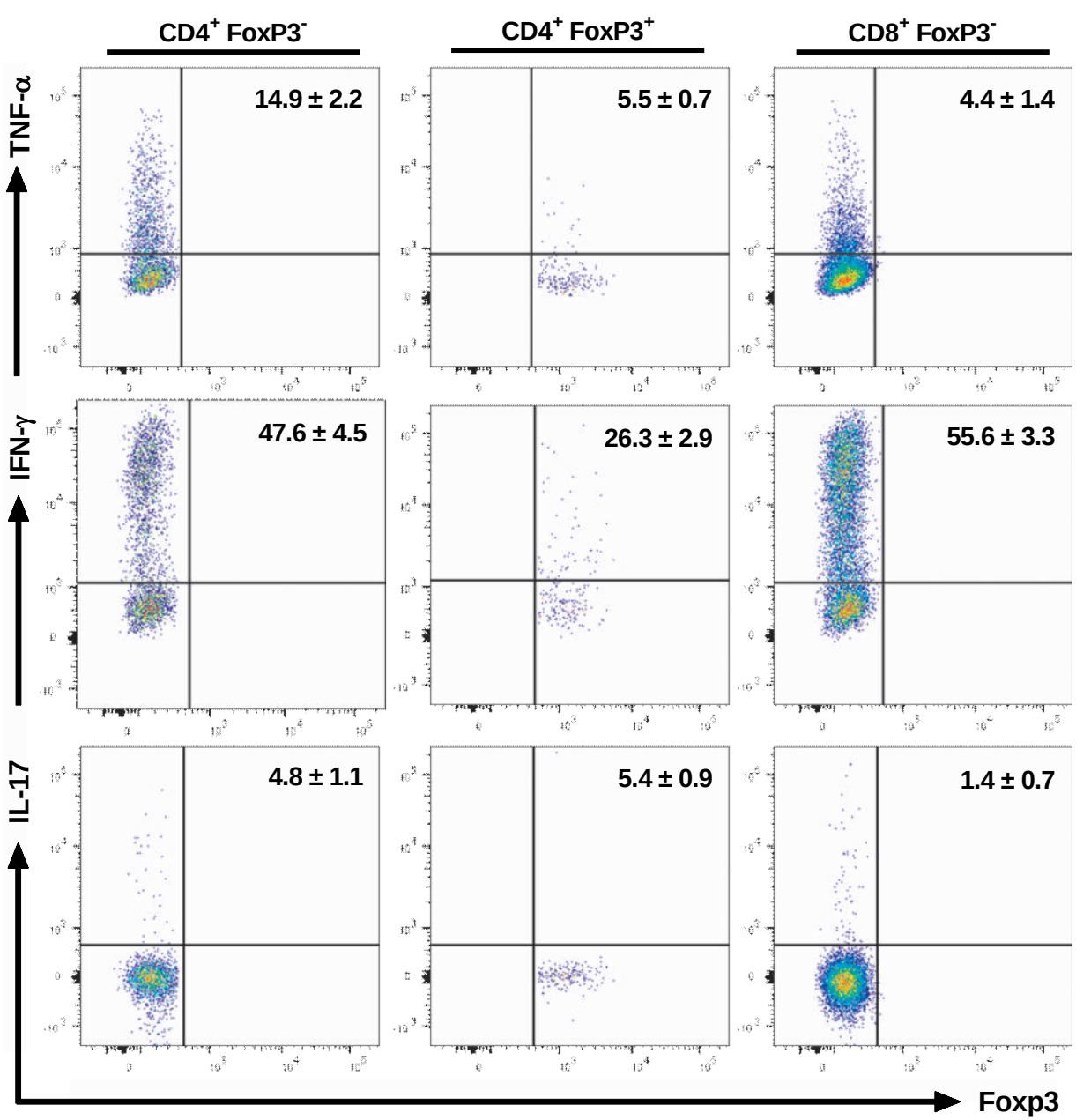

Supplemental figure 7

IL-2/anti-IL-2 complexes inhibit pro-inflammatory cytokines production by regulatory T cells after HSCT.

B6C3F1 mice were lethally irradiated and grafted as for figures 2 and 3 and were either untreated (n=14) or treated from d0 to d4 after HSCT with Cx25 (n=16) or with Cx122 (n=17). On d12, mice were sacrificed and splenocytes were collected and then stimulated with PMA/ionomycin and golgi plug for 5 hours before analysis by flow cytometry. Gating strategy of TNF-α, IFN-γ and IL-17 expression in CD4+Foxp3-, CD4+Foxp3+ and CD8+Foxp3- T cells analyzed by flow cytometry.

Supplemental figure 8

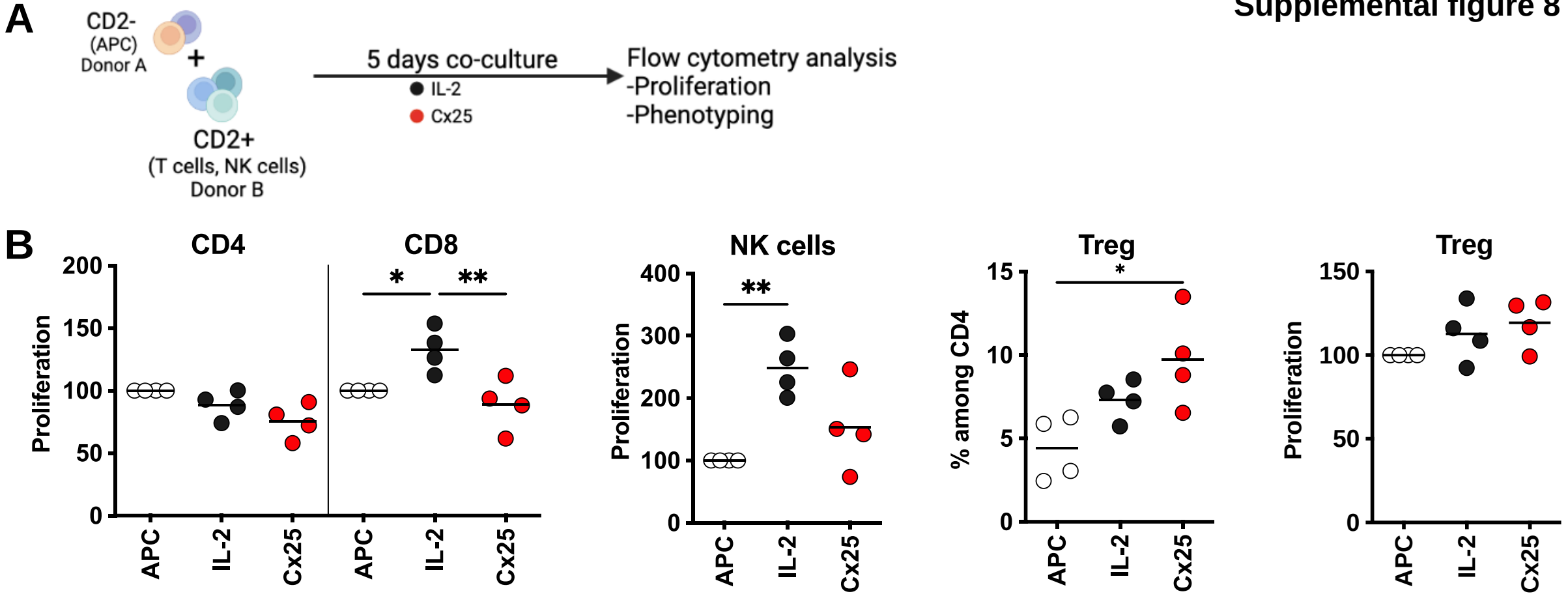

Cx25 induces human Treg expansion in vitro after an allogeneic stimulation.

(**A**) 1 x 10^6 $CD2^+$ sorted cells were stained with the cell proliferation dye and cultured with 1x10^6 allogeneic APCs ($CD2^-$ sorted cells) in the presence of IL-2 or Cx25. (**B**) At day 5, $CD4^+$, $CD8^+$ T cells, $CD56^+$ NK cell and Treg proliferations were evaluated in both $CD4^+$ and $CD8^+$ T cells and in NK cells. Treg proportion is defined by $CD25^+Foxp3^+$ expression among $CD4^+$ T cells. Dot blot sum the data of two independent experiments. Kruskal-Wallis tests were performed. *P < 0.05, **P < 0.01.

Supplemental figure 9

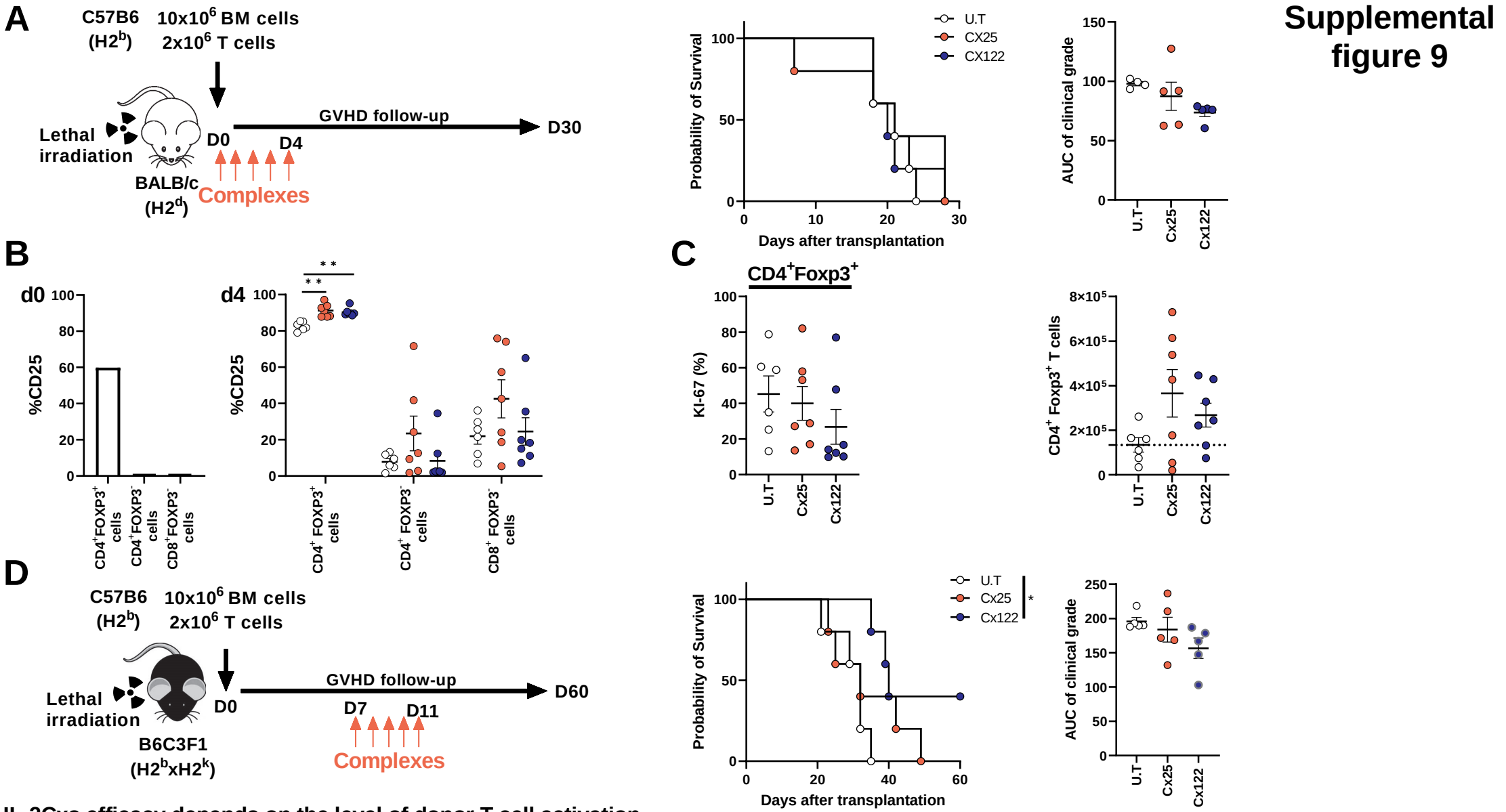

IL-2Cxs efficacy depends on the level of donor T cell activation.

(**A**) Lethally irradiated BALB/c mice received allogeneic HSCT (10 x 10^6 BM cells plus 2 x 10^6 T cells) collected from B6 mice. Mice were untreated (n=4) or treated from d0 to d4 after HSCT with Cx25 (n=5) or with Cx122 (n=5). Survival curves (left) and area under the curve (AUC) of GVHD manifestations are evaluated for each mouse for all the duration of the experiment as for Figure 1. (**B** and **C**) Lethally irradiated B6C3F1 received semi-allogeneic HSCT (10 x 10^6 BM cells plus 2 x 10^6 T cells) as in Figure 1. Before infusion, CD25 expression was assessed on donor T cells (left). Mice were sacrificed at d4, spleen cells were collected and evaluated for CD25 expression on T cells; untreated mice (n=6), Cx25 (n=7) and Cx122 (n=7). (**D**) Lethally irradiated B6C3F1 received semi-allogeneic HSCT (10 x 10^6 BM cells plus 2 x 10^6 T cells) as in Figure 1. Mice were untreated (n=5) or treated from d7 to d11 after HSCT with Cx25 (n=5) or with Cx122 (n=5).